THE ASTROPHYSICAL JOURNAL, 195:255–268, 1975 January 15


# SPECTROPHOTOMETRY OF FAINT CLUSTER GALAXIES AND THE HUBBLE DIAGRAM: AN APPROACH TO COSMOLOGY

JAMES E. GUNN AND J. B. OKE
Hale Observatories, California Institute of Technology, Carnegie Institution of Washington
*Received 1974 June 10*

## ABSTRACT

New spectrophotometric data are presented for large-redshift galaxies in clusters. A new approach to aperture corrections and the analysis of the Hubble diagram is outlined, including the explicit incorporation of evolutionary effects. The importance of selection effects on the usual methods of analysis are in principle overcome in the analysis, although the heterogeneity of the sample still makes conclusions about cosmology slightly suspect. Formal values of the deceleration parameter are derived under several sets of assumptions, yielding results between $q_0 = +0.33$ and $q_0 = -1.27$ with formal standard deviations of order 0.7.

*Subject headings:* cosmology — galaxies, clusters of — galaxies, photometry of

## I. INTRODUCTION

It has long been recognized (Humason, Mayall, and Sandage 1956) that a very powerful probe for observational cosmology is the redshift-magnitude relation defined by the brightest members of clusters of galaxies. A fundamental limitation on the use of the technique has for years been that image-tube or photographic spectra are inadequate to determine redshifts for galaxies with absorption-line spectra which are much fainter than $V = 18$, because the surface brightness of the galaxy becomes less than that of the night sky and sufficiently accurate sky subtraction is not possible photographically. The amazing determination of $z = 0.461$ for 3C 295 by Minkowski (1960) was made possible because of the presence of very strong [O II] $\lambda$3727 emission. The construction of the Palomar multichannel spectrometer (Oke 1969), with its facility to subtract the sky background accurately, has made it possible to extend redshift measurements to galaxies as faint as $V = 21$, and this paper reports on some preliminary work on such objects.

Another problem with the construction of the $(m, z)$-diagram is finding suitable candidates for measurement. We shall show in § V that selection effects can be very important in the interpretation of the data, and it is imperative that the selection criteria be reasonably well defined if any significance at all is to be attached to the results. We have therefore begun a systematic photographic search for faint clusters, and many of the new redshifts reported on here are from this sample. A much deeper survey with the Hale telescope is now under way, but as yet so few redshifts are available for this new faint sample that it will not be discussed in this paper.

In § IV we present a new technique for analyzing the $(m, z)$-diagram, which we feel properly accounts for the effects of selection and in particular for the existence of a magnitude cutoff in the data; it also allows one to take explicit account of the aperture corrections (Sandage 1972*a*) and to plot a Hubble diagram which is correct for all $q_0$.

The effects of brightness evolution are briefly considered in the last section; we find that uncertainties in the evolution are comparable to statistical uncertainties at present, but with very much fainter samples they will completely dominate.

## II. OBSERVATIONAL MATERIAL

The distant clusters of galaxies for which detailed observations of individual galaxies have been obtained are listed in the lower part of table 1 under code numbers 1–28 along with their 1950 coordinates, which should be accurate to $0^m1$ and 1′, respectively, and the galactic latitude $b^{II}$. The various objects will usually be referred to by their code numbers. Many of the galaxies—namely, 10, 11, 12, 14, 16, 17, 19, 20, 22, and 27—come from a 48-inch (122-cm) Schmidt survey made on IIIa-J plates, and were found under reasonably controlled conditions. Six of these new clusters are shown in figure 1 (plate 1). Three others—13, 15, and 21—are the brightest members of clusters found in a search for quasar-cluster association by one of us (J. E. G.) on deep IIIa-J plates taken with the 48-inch Palomar Schmidt. No. 13 is in Zwicky's catalog of clusters of galaxies (Zwicky, Karpowicz, and Kowal 1965). The cluster 1021.1+0427 (No. 18) was found by Zwicky (private communication), clusters 1446.7+2621 (Nos. 23 and 24) and cluster 0024.0+1653 (Nos. 26 and 27) were discovered by Humason and Sandage (1957), and, of course, 3C 295 (No. 28) was first observed optically by Minkowski (1960). The further objects, Nos. 5 and 8, are foreground galaxies which were observed even though it was anticipated that such was the case. Number 5, a galaxy very near to 3C 295, was mentioned by Minkowski (1960). Number 8 is in front of the cluster 1446.7+2621. Numbers 1, 2, 3, and 6 are well-known clusters (Humason, Mayall, and Sandage 1956). The individual galaxy numbers are taken from this paper. Finally, three Abell clusters (Abell 1958), Nos. 4, 7, and 9, are included. For reasons discussed below, not all of these objects have been used in the final analysis.

## TABLE 1

### DATA ON CLUSTERS OF GALAXIES

| Code | Object | α(1950) | δ(1950) | bII | Apert. | V | Red Cor. | Radius | Ap. Cor. | K Cor. | VI | log z | z | Remarks |
|---|---|---|---|---|---|---|---|---|---|---|---|---|---|---|
| P | Abell 1060 | 10 34.5 | -27 16 | +26 | 122.00 | 11.60 | 0.26 | 17.94 | +0.09 | 0.03 | 11.39 | -1.907 | 0.012 | |
| P | Abell 194 | 01 23.0 | -01 46 | -63 | 79.90 | 12.34 | 0.00 | 16.71 | +0.04 | 0.05 | 12.32 | -1.750 | 0.018 | |
| P | Abell 779 | 09 16.8 | +34 00 | +44 | 70.80 | 13.21 | 0.05 | 16.66 | +0.04 | 0.05 | 13.13 | -1.697 | 0.020 | |
| P | Abell 1367 | 11 41.9 | +20 07 | +73 | 69.80 | 12.56 | 0.00 | 16.66 | +0.04 | 0.05 | 12.53 | -1.690 | 0.020 | |
| S | Coma | 12 57.4 | +28 15 | +88 | 68.80 | 12.01 | 0.00 | 17.81 | +0.09 | 0.06 | 12.13 | -1.654 | 0.022 | A |
| P | Abell 400 | 02 55.0 | +05 50 | -44 | 64.60 | 13.21 | 0.05 | 17.38 | +0.07 | 0.06 | 13.15 | -1.636 | 0.023 | |
| P | Abell 634 | 08 10.5 | +58 13 | +34 | 54.10 | 13.61 | 0.15 | 16.66 | +0.04 | 0.07 | 13.41 | -1.575 | 0.027 | |
| P | Abell 2666 | 23 48.4 | +26 53 | -34 | 52.80 | 12.95 | 0.15 | 16.67 | +0.04 | 0.07 | 12.75 | -1.564 | 0.027 | |
| S | Abell 1213 | 11 13.8 | +29 33 | +69 | 37.60 | 14.28 | 0.00 | 12.45 | -0.18 | 0.08 | 14.11 | -1.542 | 0.029 | |
| P | Abell 2634 | 23 35.8 | +26 45 | -33 | 46.40 | 13.22 | 0.16 | 16.68 | +0.04 | 0.08 | 13.00 | -1.504 | 0.031 | |
| S | Abell 2199 | 16 26.9 | +39 38 | +44 | 55.10 | 12.78 | 0.05 | 19.20 | +0.15 | 0.08 | 12.88 | -1.519 | 0.030 | |
| P | Abell 2162 | 16 10.5 | +29 40 | +46 | 45.70 | 13.48 | 0.04 | 16.67 | +0.04 | 0.08 | 13.39 | -1.498 | 0.032 | |
| P | Abell 2197 | 16 26.5 | +41 01 | +43 | 45.10 | 13.20 | 0.06 | 16.65 | +0.04 | 0.08 | 13.08 | -1.492 | 0.032 | |
| P | Abell 1257 | 11 23.4 | +35 37 | +70 | 43.00 | 14.52 | 0.00 | 16.67 | +0.04 | 0.09 | 14.46 | -1.470 | 0.034 | |
| P | Abell 1228 | 11 18.9 | +34 37 | +69 | 42.40 | 14.10 | 0.00 | 16.66 | +0.04 | 0.09 | 14.04 | -1.463 | 0.034 | |
| S | Hercules | 16 03.0 | +17 53 | +44 | 42.30 | 14.00 | 0.05 | 16.76 | +0.04 | 0.09 | 13.99 | -1.460 | 0.035 | A |
| P | Abell 1185 | 11 08.2 | +28 57 | +68 | 41.80 | 13.58 | 0.00 | 16.65 | +0.04 | 0.09 | 13.51 | -1.457 | 0.035 | |
| S | Abell 2052 | 15 14.3 | +07 12 | +50 | 48.30 | 13.62 | 0.00 | 19.34 | +0.15 | 0.09 | 13.77 | -1.455 | 0.035 | |
| P | Abell 2147 | 16 00.0 | +16 03 | +45 | 41.60 | 13.86 | 0.04 | 16.66 | +0.04 | 0.09 | 13.75 | -1.455 | 0.035 | |
| P | Abell 76 | 00 37.2 | +06 30 | -56 | 38.90 | 13.83 | 0.00 | 16.66 | +0.04 | 0.10 | 13.76 | -1.424 | 0.038 | |
| P | Abell 1139 | 10 55.5 | +01 47 | +53 | 39.00 | 14.20 | 0.00 | 16.91 | +0.05 | 0.10 | 14.14 | -1.418 | 0.038 | |
| S | Abell 119 | 00 53.9 | -01 32 | -64 | 30.60 | 14.21 | 0.00 | 13.43 | -0.13 | 0.10 | 14.07 | -1.412 | 0.039 | |
| P | Abell 548 | 05 45.1 | -15 38 | -25 | 37.60 | 14.13 | 0.28 | 16.66 | +0.04 | 0.10 | 13.77 | -1.408 | 0.039 | |
| P | Abell 576 | 07 17.4 | +55 51 | +26 | 36.50 | 14.37 | 0.26 | 16.67 | +0.04 | 0.11 | 14.03 | -1.394 | 0.040 | |
| P | Abell 2657 | 23 42.3 | +08 53 | -50 | 35.30 | 14.77 | 0.00 | 16.28 | +0.02 | 0.11 | 14.67 | -1.389 | 0.041 | |
| S | Peg II | 23 07.9 | +07 20 | -48 | 35.20 | 14.26 | 0.02 | 16.97 | +0.05 | 0.11 | 14.27 | -1.369 | 0.043 | A |
| P | Abell 1736 | 13 24.1 | -26 52 | +35 | 34.40 | 14.33 | 0.14 | 16.69 | +0.04 | 0.11 | 14.10 | -1.366 | 0.043 | |
| S | Cl 2322+1425 | 23 22.1 | +14 24 | -43 | 35.20 | 14.49 | 0.06 | 17.37 | +0.07 | 0.12 | 14.47 | -1.358 | 0.044 | A |
| P | Abell 2152 | 16 03.1 | +17 53 | +44 | 33.70 | 14.40 | 0.05 | 16.67 | +0.04 | 0.12 | 14.26 | -1.357 | 0.044 | |
| P | Abell 147 | 01 05.6 | +01 55 | -60 | 33.60 | 14.74 | 0.00 | 16.65 | +0.04 | 0.12 | 14.65 | -1.356 | 0.044 | |
| P | Abell 671 | 08 25.4 | +30 36 | +33 | 30.10 | 14.23 | 0.16 | 16.65 | +0.04 | 0.13 | 13.96 | -1.304 | 0.050 | |
| S | Cl 1145+5559 | 11 44.7 | +56 01 | +59 | 30.60 | 14.74 | 0.00 | 17.52 | +0.08 | 0.14 | 14.77 | -1.287 | 0.052 | A |
| P | Abell 151 | 01 06.4 | -15 41 | -78 | 28.60 | 14.29 | 0.00 | 16.67 | +0.04 | 0.14 | 14.18 | -1.279 | 0.053 | |
| P | Abell 993 | 10 19.4 | -04 42 | +42 | 28.40 | 14.48 | 0.07 | 16.67 | +0.04 | 0.14 | 14.30 | -1.276 | 0.053 | |
| P | Abell 754 | 09 06.4 | -09 27 | +25 | 28.10 | 14.34 | 0.28 | 16.69 | +0.04 | 0.14 | 13.94 | -1.270 | 0.054 | |
| S | Cl 1024+1039 | 10 24.4 | +10 39 | +52 | 18.80 | 15.36 | 0.00 | 13.25 | -0.14 | 0.17 | 15.14 | -1.188 | 0.065 | A |
| S | Cl 1239+1852 | 12 38.8 | +18 52 | +81 | 18.80 | 15.06 | 0.00 | 14.49 | -0.07 | 0.19 | 14.89 | -1.144 | 0.072 | A |
| S | Abell 2670 | 23 51.6 | -10 41 | -68 | 18.80 | 15.25 | 0.00 | 15.47 | -0.02 | 0.20 | 15.14 | -1.114 | 0.077 | |
| S | Abell 2029 | 15 08.5 | +05 57 | +50 | 24.00 | 14.44 | 0.00 | 19.82 | +0.17 | 0.21 | 14.49 | -1.110 | 0.078 | |
| P | Abell 278 | 01 54.4 | +31 59 | -29 | 17.70 | 15.95 | 0.22 | 16.66 | +0.04 | 0.24 | 15.52 | -1.044 | 0.090 | |
| | | | | | | VM | | | | | | | | |
| 1 | Cr B Cl, G2 | 15 20.3 | +27 52 | +57 | 7.00 | 16.20 | | | | | | -1.142 | 0.072 | A,B |
| 2 | U Ma II Cl, Gl | 10 55.6 | +57 03 | +54 | 7.00 | 17.35 | 0.00 | 9.23 | -0.41 | | 18.05 | -0.866 | 0.136 | A |
| 3 | Cl 1534.4+3748, Gl | 15 34.4 | +37 48 | +54 | 7.00 | 17.40 | 0.00 | 10.11 | -0.34 | | 17.06 | -0.815 | 0.153 | A |
| 4 | Abell 665, Gl | 08 26.3 | +66 04 | +34 | 14.00 | 16.75 | 0.12 | 23.12 | +0.29 | | 16.92 | -0.738 | 0.183 | |
| 5 | Foreground, 3C 295 | 14 09.5 | +52 26 | +61 | 5.00 | 18.72 | | | | | | -0.721 | 0.190 | F |
| 6 | Hydra Cl, G8+G9 | 08 55.3 | +03 22 | +29 | 9.90 | 16.80 | 0.17 | 17.55 | +0.08 | | 16.71 | -0.692 | 0.202 | A,C |
| 7 | Abell 2317, Gl | 19 08.9 | +68 59 | +23 | 7.00 | 17.70 | | | | | | -0.678 | 0.210 | J |
| 8 | Foreground Cl 1446.7+2621, Gl | 14 46.7 | +26 21 | +63 | 7.00 | 19.05 | | | | | | -0.672 | 0.213 | D |
| 9 | Abell 1961, Gl | 14 42.4 | +31 25 | +64 | 9.90 | 17.17 | | | | | | -0.638 | 0.230 | J |
| 10 | Cl 1604.0+3935 | 16 04.0 | +39 35 | +49 | 7.00 | 18.15 | 0.01 | 13.76 | -0.11 | | 18.04 | -0.623 | 0.235 | |
| 11 | Cl 0025.8+0617, Gl+G2 | 00 25.8 | +06 17 | -56 | 5.00 | 19.09 | | | | | | | 0.180 | G |
| 12 | Cl 0308.5+1642 | 03 08.5 | +16 42 | -35 | 7.00 | 18.90 | 0.11 | 14.70 | -0.06 | | 18.73 | -0.585 | 0.260 | |
| 13 | Cluster near PHL 1093, G2 | 01 37.4 | +01 16 | -59 | 5.00 | 19.05 | 0.00 | 10.75 | -0.30 | | 18.75 | -0.569 | 0.270 | |
| 14 | Cl 1318.1+3157 | 13 28.1 | +31 57 | +82 | 7.00 | 18.20 | 0.00 | 15.05 | -0.04 | | 18.16 | -0.569 | 0.270 | |
| 15 | Cluster near 3C 323.1, Gl | 15 45.2 | +21 05 | +49 | 7.00 | 17.90 | 0.01 | 15.05 | -0.04 | | 17.85 | -0.569 | 0.270 | |
| 16 | Cl 1612.6+4204 | 16 12.6 | +42 04 | +49 | 7.00 | 18.80 | 0.02 | 15.22 | -0.03 | | 18.74 | -0.561 | 0.275 | |
| 17 | Cl 1607.6+3953 | 16 07.6 | +39 53 | +49 | 5.00 | 18.35 | 0.02 | 11.00 | -0.28 | | 18.05 | -0.552 | 0.280 | |
| 18 | Cl 1021.1+0427 | 10 21.1 | +04 27 | +48 | 7.00 | 17.95 | 0.01 | 15.39 | -0.02 | | 17.92 | -0.544 | 0.286 | H |
| 19 | Cl 1610.8+4115 | 16 10.8 | +41 15 | +49 | 5.00 | 18.65 | 0.02 | 11.46 | -0.25 | | 18.39 | -0.523 | 0.300 | |
| 20 | Cl 0948.8+4536 | 09 48.8 | +45 36 | +50 | 5.00 | 18.65 | 0.00 | 11.69 | -0.23 | | 18.42 | -0.516 | 0.305 | |
| 21 | Cl 1049.4-0904, Gl | 10 49.4 | -09 04 | +43 | 5.00 | 19.00 | 0.04 | 12.11 | -0.20 | | 18.75 | -0.482 | 0.330 | |
| 22 | Cl 0948.9+4426 | 09 48.9 | +44 26 | +50 | 7.00 | 18.45 | 0.00 | 17.78 | +0.09 | | 18.54 | -0.442 | 0.361 | |
| 23 | Cl 1446.7+2621, G3 | 14 46.7 | +26 21 | +63 | 7.00 | 19.10 | | | | | | -0.438 | 0.365 | D |
| 24 | Cl 1446.7+2621, G4 | 14 46.7 | +26 21 | +63 | 7.00 | 18.75 | 0.00 | 18.11 | +0.10 | | 18.85 | -0.428 | 0.373 | D |
| 25 | Cl 0949.9+4409 | 09 49.9 | +44 09 | +50 | 5.00 | 19.40 | 0.00 | 13.15 | -0.14 | | 19.26 | -0.414 | 0.385 | |
| 26 | Cl 0024.0+1653, Gl | 00 24.0 | +16 53 | -45 | 7.00 | 18.35 | 0.03 | 18.29 | +0.11 | | 18.43 | -0.420 | 0.380 | D,E |
| 27 | Cl 0024.0+1653, G3 | 00 24.0 | +16 53 | -45 | 7.00 | 18.70 | | | | | | -0.389 | 0.408 | D,E |
| 28 | 3C 295 | 14 09.5 | +52.26 | +61 | 7.00 | 18.10 | 0.00 | 20.13 | +0.18 | | 18.28 | -0.332 | 0.465 | F |

### NOTES TO TABLE 1

A. See Humason *et al.* 1956.
B. Measuring aperture too small to make reliable aperture corrections. Not used in analysis.
C. Pair of bright galaxies in aperture. See text for comments on such systems.
D. See Humason and Sandage 1957.
E. Photograph of cluster published by Zwicky 1959.
F. See Minkowski 1960.
G. Small group of spirals, not used in analysis.
H. Cluster discovered by Zwicky (private communication).
J. From a sample of cD galaxies. Not used in analysis (see text).

TABLE 2

FAINT GALAXY SPECTRAL ENERGY DISTRIBUTIONS IN AB

| log ν | 5 | 7 | 9 | 10 | 11 | 12 | 14 | 16 | 17 | 18 | 19 | 20 | 22 | 25 |
|---|---|---|---|---|---|---|---|---|---|---|---|---|---|---|
| 14.964 | 20.89 | ... | ... | ... | ... | 21.35 | ... | ... | ... | 20.30 | ... | 21.19 | ... | ... |
| .953 | 20.08 | ... | ... | ... | ... | 21.97 | ... | ... | ... | 19.63 | ... | * | ... | ... |
| .943 | 21.28 | ... | ... | ... | ... | * | ... | ... | ... | 19.70 | ... | 22.41 | ... | ... |
| .933 | 21.39 | ... | ... | ... | ... | 21.88 | ... | ... | ... | 19.88 | ... | * | 22.62 | ... |
| .923 | * | ... | 19.91 | ... | ... | 21.69 | ... | ... | ... | 19.96 | ... | 21.93 | * | ... |
| .913 | 22.10 | ... | 19.40 | 20.95 | ... | 21.86 | ... | ... | ... | 19.83 | ... | 23.60 | 21.25 | ... |
| .904 | * | 21.11 | 20.24 | 21.20 | ... | 21.56 | ... | ... | ... | 19.85 | ... | 21.70 | 22.63 | ... |
| .896 | 20.44 | 20.46 | 20.15 | 20.69 | ... | 22.28 | 20.45 | ... | ... | 19.50 | ... | 21.76 | 21.71 | ... |
| .886 | * | 20.11 | 19.52 | 21.27 | ... | 22.02 | 20.60 | ... | ... | 19.76 | ... | 22.33 | 22.20 | ... |
| .877 | 21.44 | 20.80 | 20.38 | 20.61 | 20.91 | 21.53 | 20.53 | 20.95 | 21.34 | 19.75 | 21.47 | 21.98 | 21.63 | 22.48 |
| .868 | 23.07 | 19.68 | 19.48 | 21.41 | 22.18 | 21.64 | 20.96 | 21.45 | 23.21 | 19.47 | 21.61 | 21.36 | 21.76 | 21.98 |
| .860 | 20.74 | 20.29 | 19.59 | 20.40 | 21.51 | 21.19 | 20.74 | 21.18 | 21.75 | 19.57 | 21.00 | 21.60 | 21.25 | 23.06 |
| .852 | 21.10 | 19.87 | 19.36 | 20.57 | 21.22 | 21.16 | 20.85 | 20.86 | 21.23 | 19.66 | 21.19 | 21.24 | 21.74 | 22.30 |
| .843 | 21.22 | 19.95 | 19.94 | 20.44 | 21.11 | 21.13 | 21.15 | 21.94 | 20.68 | 19.46 | 21.60 | 21.22 | 21.00 | 22.24 |
| .836 | 20.46 | 20.29 | 19.34 | 20.51 | 19.95 | 21.11 | 20.65 | 21.09 | 20.56 | 19.40 | 20.93 | 20.66 | 21.16 | 23.12 |
| .828 | 20.60 | 19.84 | 18.95 | 20.33 | 20.94 | 21.31 | 20.50 | 20.65 | 20.76 | 19.49 | 20.63 | 21.03 | 20.78 | 23.18 |
| .820 | 20.51 | 19.48 | 19.41 | 20.00 | 21.20 | 21.04 | 20.29 | 20.53 | 20.73 | 19.49 | 20.62 | 21.34 | 21.53 | 21.56 |
| .812 | 20.92 | 19.68 | 18.92 | 20.18 | 20.86 | 20.62 | 20.18 | 20.82 | 20.78 | 19.22 | 20.50 | 20.96 | 21.25 | 22.32 |
| .805 | 20.46 | 19.53 | 19.27 | 20.11 | 20.54 | 20.62 | 20.05 | 20.78 | 20.80 | 19.05 | 20.67 | 20.71 | 20.89 | 21.70 |
| .797 | 19.87 | 19.72 | 18.68 | 20.04 | 20.21 | 20.56 | 19.94 | 20.78 | 20.05 | 17.72 | 20.59 | 20.26 | 20.51 | 24.24 |
| .790 | 19.34 | 18.87 | 18.81 | 20.00 | 20.02 | 20.45 | 20.62 | 21.12 | 19.93 | 18.92 | 20.25 | 20.88 | 20.15 | 21.03 |
| .783 | 19.61 | 18.79 | 18.36 | 19.37 | 20.19 | 20.20 | 19.84 | 21.38 | 20.46 | 18.94 | 20.43 | 20.64 | 20.57 | 21.59 |
| .776 | 19.59 | 18.88 | 18.31 | 19.26 | 20.27 | 20.11 | 19.64 | 20.74 | 20.29 | 18.63 | 20.82 | 20.70 | 20.48 | 21.41 |
| .769 | 19.51 | 18.82 | 18.30 | 19.30 | 19.96 | 19.77 | 19.12 | 20.15 | 20.63 | 18.68 | 20.20 | 20.45 | 20.18 | 21.39 |
| .763 | 19.28 | 18.69 | 18.50 | 19.33 | 19.83 | 19.90 | 19.60 | 19.71 | 19.94 | 18.68 | 19.89 | 20.29 | 20.40 | 21.24 |
| .756 | 19.41 | 18.59 | 18.24 | 19.19 | 19.83 | 19.80 | 19.44 | 19.83 | 19.52 | 18.79 | 19.91 | 19.86 | 20.16 | 21.06 |
| .749 | 19.35 | 18.43 | 18.07 | 18.96 | 19.72 | 19.85 | 19.31 | 19.82 | 19.61 | 18.80 | 19.74 | 19.63 | 20.23 | 21.05 |
| .743 | 19.34 | 18.29 | 17.74 | 18.82 | 19.74 | 19.78 | 19.44 | 19.74 | 19.60 | 18.66 | 19.65 | 19.93 | 19.80 | 21.11 |
| .737 | 19.16 | 18.24 | 17.79 | 18.74 | 19.45 | 19.55 | 19.16 | 19.28 | 19.54 | 18.92 | 19.66 | 19.76 | 19.58 | 20.98 |
| .730 | 19.26 | 18.10 | 17.66 | 18.80 | 19.57 | 19.51 | 18.95 | 19.69 | 19.38 | 18.45 | 19.47 | 19.66 | 19.54 | 20.43 |
| .724 | 19.10 | 18.13 | 17.58 | 18.70 | 19.45 | 19.47 | 18.74 | 19.58 | 19.21 | 18.56 | 19.67 | 19.63 | 19.66 | 20.79 |
| .717 | 18.98 | 18.00 | 17.64 | 18.64 | 19.36 | 19.35 | 18.69 | 19.46 | 19.27 | 18.46 | 19.35 | 19.43 | 19.72 | 20.38 |
| .705 | 18.76 | 17.97 | 17.50 | 18.60 | 19.35 | 19.41 | 18.72 | 19.39 | 18.95 | 18.37 | 19.19 | 19.28 | 19.58 | 20.53 |
| .693 | 18.81 | 17.99 | 17.41 | 18.53 | 19.19 | 19.22 | 18.42 | 18.98 | 18.66 | 18.42 | 19.04 | 19.11 | 19.13 | 20.19 |
| .682 | 18.74 | 17.90 | 17.20 | 18.45 | 19.12 | 19.03 | 18.41 | 19.16 | 18.67 | 17.85 | 18.93 | 18.97 | 18.99 | 19.74 |
| .671 | 18.68 | 17.72 | 17.48 | 18.38 | 19.06 | 19.07 | 18.40 | 19.05 | 18.66 | 17.96 | 19.00 | 18.91 | 18.93 | 19.69 |
| .660 | 18.68 | 17.65 | 17.20 | 18.20 | 19.12 | 19.07 | 18.41 | 19.21 | 18.72 | 18.01 | 18.98 | 18.86 | 18.78 | 19.78 |
| .650 | 18.70 | 17.56 | 17.19 | 18.20 | 18.95 | 18.92 | 18.34 | 19.17 | 18.59 | 18.06 | 19.03 | 18.95 | 18.93 | 19.75 |
| .639 | 18.79 | 17.54 | 17.16 | 18.20 | 18.75 | 18.89 | 18.09 | 18.80 | 18.63 | 18.13 | 19.11 | 18.92 | 18.76 | 19.73 |
| .629 | 18.54 | 17.42 | 17.07 | 18.08 | 18.74 | 18.72 | 18.11 | 18.86 | 18.42 | 18.07 | 18.66 | 18.62 | 18.82 | 19.72 |
| .620 | 18.55 | 17.41 | 17.00 | 18.00 | 18.64 | 18.63 | 18.01 | 18.77 | 18.29 | 17.96 | 18.67 | 18.54 | 18.54 | 19.71 |
| .610 | 18.31 | 17.32 | ... | 17.97 | 18.64 | 18.57 | ... | 18.49 | 18.32 | 17.75 | 18.57 | 18.54 | 18.30 | 19.44 |
| .601 | 18.30 | 17.44 | 16.88 | 17.96 | 18.57 | 18.58 | 17.95 | 18.54 | 18.16 | 17.87 | 18.64 | 18.50 | 18.46 | 19.46 |
| .592 | 18.37 | 17.20 | ... | 17.90 | 18.48 | 18.60 | ... | 18.46 | 18.21 | 17.79 | 18.55 | 18.63 | 18.42 | 19.37 |
| .583 | 18.43 | 17.13 | 16.94 | 17.79 | 18.55 | 18.52 | 17.90 | 18.45 | 18.24 | 17.74 | 18.67 | 18.42 | 17.80 | 19.28 |
| .574 | 18.67 | 17.14 | 16.63 | 17.77 | 18.52 | 18.44 | 17.69 | 18.72 | 18.06 | 17.71 | 18.49 | 18.28 | 18.37 | 19.29 |
| .565 | 18.21 | 16.97 | 16.38 | 17.72 | 18.34 | 18.32 | 18.25 | 18.15 | 17.88 | 17.05 | 18.27 | 18.38 | 18.33 | 19.22 |
| .557 | 18.56 | 16.96 | 16.88 | 17.48 | 18.14 | 18.17 | 17.48 | 18.89 | 17.71 | 17.45 | 18.18 | 18.16 | 18.19 | 18.87 |
| .549 | 18.10 | 17.04 | 16.44 | 17.60 | 18.32 | 18.32 | 17.35 | 17.93 | 18.11 | 15.98 | 18.84 | 18.06 | 17.44 | 19.42 |
| .540 | 19.25 | 17.38 | 16.35 | 17.70 | 18.34 | 18.12 | 17.30 | 18.26 | 18.14 | 16.79 | 18.22 | 18.04 | 18.10 | 19.43 |
| .533 | 18.08 | 16.91 | ... | 17.59 | 18.37 | 18.34 | ... | 18.49 | 17.82 | 17.32 | 18.41 | 18.16 | 17.80 | 18.94 |
| .525 | 17.91 | 16.92 | 16.63 | 17.69 | 18.51 | 18.74 | 17.38 | 18.12 | 17.85 | 17.58 | 18.02 | 18.14 | 19.00 | 19.13 |
| .517 | 18.55 | 16.77 | ... | 17.38 | 18.01 | 18.20 | ... | 18.27 | 17.51 | 17.55 | 18.11 | 18.13 | 18.11 | 19.17 |
| .509 | 18.11 | 16.92 | 16.39 | 17.40 | 17.62 | 18.08 | 19.18 | 18.06 | 17.82 | 17.50 | 18.21 | 18.18 | 16.93 | 18.82 |
| .502 | * | 16.86 | 16.19 | 17.38 | 17.95 | 17.76 | 18.42 | 17.92 | 17.73 | 16.40 | 18.05 | 17.87 | 17.25 | 19.33 |
| .495 | 18.43 | 16.69 | 16.17 | 17.34 | 18.22 | 18.24 | 17.11 | 17.45 | 18.26 | 17.06 | 18.16 | 17.80 | 17.78 | 18.64 |
| .488 | 17.31 | ... | 16.30 | 17.51 | 17.97 | 18.00 | 17.38 | 17.68 | 17.63 | 17.20 | 18.21 | 18.08 | 18.52 | 19.40 |
| .480 | 17.84 | 16.54 | 16.27 | 17.12 | 17.88 | 17.99 | 17.22 | 18.33 | 17.62 | 17.04 | 18.31 | 17.77 | 16.94 | 19.06 |
| .473 | 17.43 | 16.42 | 16.55 | 16.93 | 17.73 | 17.39 | 17.86 | 18.15 | 17.03 | 16.73 | 18.43 | 17.90 | 17.31 | 18.63 |
| .467 | 17.26 | 16.61 | ... | 17.45 | 17.59 | 18.20 | ... | 17.55 | 17.36 | 17.21 | 17.82 | 17.41 | 17.81 | 19.53 |
| .460 | 18.16 | 16.59 | 16.19 | 17.69 | 18.10 | 18.83 | 17.52 | 17.88 | 17.40 | 17.07 | 17.82 | 17.62 | 18.36 | 17.92 |
| 14.453 | 17.79 | 16.95 | ... | 17.16 | 18.19 | ... | ... | ... | 17.32 | 17.34 | 17.62 | 17.66 | ... | ... |

## TABLE 3

### FAINT GALAXY SPECTRAL ENERGY DISTRIBUTIONS IN AB

| log ν | 1 | 2 | 3 | 4 | 8 | 15 | 23 | 24 | 26 | 27 | 28 | log ν | 13 |
|---|---|---|---|---|---|---|---|---|---|---|---|---|---|
| 14.956 | ... | 19.16 | 19.78 | ... | ... | ... | ... | ... | ... | ... | ... | 14.964 | 21.84 |
| .945 | 18.92 | 19.26 | 20.47 | ... | ... | ... | ... | ... | ... | ... | ... | .943 | 20.67 |
| .935 | 19.47 | 19.58 | 20.08 | ... | 20.57 | ... | ... | ... | ... | ... | ... | .923 | 21.09 |
| .926 | 19.25 | 19.03 | 20.92 | ... | 20.86 | ... | ... | ... | ... | ... | ... | .904 | 21.31 |
| .916 | 19.06 | 19.31 | 20.30 | ... | 21.55 | ... | ... | ... | ... | ... | ... | .886 | 21.28 |
| .906 | 18.63 | 19.08 | 20.30 | 19.38 | 22.27 | ... | ... | ... | ... | ... | ... | .868 | 21.21 |
| .897 | 18.77 | 19.06 | 19.93 | 19.26 | 21.91 | ... | 22.82 | ... | ... | ... | ... | .851 | 21.62 |
| .888 | 18.64 | 19.01 | 19.72 | 19.67 | 21.69 | ... | 22.39 | ... | ... | ... | ... | .835 | 21.12 |
| .879 | 18.32 | 18.76 | 19.84 | 19.51 | 21.03 | 21.01 | 22.93 | 21.87 | 21.92 | ... | 21.60 | .820 | 21.10 |
| .871 | 18.26 | 18.66 | 19.78 | 19.51 | 21.02 | 21.51 | 21.90 | 24.56 | 21.96 | 23.14 | 21.97 | .805 | 21.33 |
| .862 | 18.36 | 18.57 | 19.93 | 19.18 | 21.75 | 20.93 | 21.78 | 22.19 | 21.81 | 21.57 | 22.11 | .790 | 20.48 |
| .854 | 18.10 | 18.51 | 19.46 | 19.08 | 20.84 | 20.36 | 22.29 | 21.70 | 22.07 | 21.58 | 21.80 | .776 | 20.57 |
| .845 | 17.71 | 18.10 | 19.51 | 19.22 | 21.19 | 20.29 | 21.99 | 21.99 | 21.81 | 21.61 | 21.67 | .762 | 20.18 |
| .837 | 17.43 | 18.13 | 19.52 | 18.73 | 20.78 | 20.04 | 21.38 | 22.73 | 21.56 | 21.65 | 21.42 | .749 | 20.31 |
| .830 | 17.39 | 18.19 | 19.49 | 18.81 | 20.68 | 19.88 | 22.21 | 21.89 | 21.34 | 21.09 | 21.31 | .736 | 19.90 |
| .822 | 17.28 | 18.09 | 19.30 | 19.00 | 20.68 | 20.01 | 21.34 | 21.50 | 21.17 | 21.07 | 21.36 | .724 | 19.51 |
| .814 | 17.23 | 18.02 | 18.82 | 18.75 | 20.78 | 20.09 | 21.80 | 21.83 | 20.73 | 20.95 | 21.00 | .709 | 19.58 |
| .807 | 17.01 | 17.87 | 18.60 | 18.89 | 20.83 | 19.74 | 21.26 | 21.09 | 20.86 | 21.05 | 20.67 | .683 | 19.35 |
| .799 | 16.85 | 17.87 | 18.64 | 18.05 | 20.90 | 19.82 | 21.34 | 21.31 | 21.11 | 21.20 | 20.69 | .659 | 19.36 |
| .792 | 16.74 | 17.86 | 18.56 | 18.01 | 20.76 | 19.92 | 21.11 | 21.32 | 20.71 | 20.94 | 20.60 | .635 | 19.23 |
| .785 | 16.59 | 17.75 | 18.48 | 17.96 | 20.14 | 19.78 | 21.28 | 20.86 | 20.82 | 20.56 | 20.59 | .613 | 18.81 |
| .778 | 16.61 | 17.64 | 18.32 | 17.91 | 19.96 | 19.88 | 20.76 | 21.08 | 20.80 | 20.79 | 20.55 | .593 | 18.59 |
| .771 | 16.55 | 17.69 | 18.23 | 17.84 | 19.93 | 19.25 | 21.27 | 20.80 | 20.22 | 20.38 | 20.36 | .573 | 18.41 |
| .764 | 16.50 | 17.64 | 18.03 | 17.69 | 20.14 | 19.11 | 21.20 | 20.77 | 20.60 | 20.51 | 20.17 | .554 | 18.18 |
| .758 | 16.46 | 17.53 | 17.92 | 17.47 | 20.03 | 19.04 | 20.98 | 20.70 | 20.33 | 20.41 | 20.32 | .535 | 17.94 |
| .751 | 16.44 | 17.52 | 17.84 | 17.35 | 19.70 | 19.02 | 20.94 | 20.71 | 20.36 | 20.30 | 20.20 | .518 | 18.48 |
| .745 | 16.47 | 17.57 | 17.90 | 17.32 | 19.75 | 18.84 | 20.61 | 20.61 | 20.17 | 20.28 | 19.85 | .501 | 17.86 |
| .738 | 16.36 | 17.62 | 17.68 | 17.17 | 19.63 | 18.74 | 20.60 | 20.18 | 19.89 | 20.63 | 19.52 | .485 | 17.64 |
| .732 | 16.53 | 17.46 | 17.72 | 17.31 | 19.49 | 18.77 | 20.04 | 19.86 | 19.77 | 20.23 | 19.99 | .469 | 16.92 |
| .726 | 16.25 | 17.40 | 17.71 | 17.06 | 19.43 | 18.60 | 20.14 | 20.07 | 19.57 | 19.70 | 19.82 | .454 | 16.85 |
| .720 | 16.19 | 17.45 | 17.69 | 17.32 | 19.44 | 18.52 | 20.14 | 19.66 | 19.46 | 19.60 | 19.90 | | |
| .714 | 16.15 | 17.41 | 17.62 | 17.10 | 19.16 | 18.40 | 20.22 | 19.77 | 19.55 | 19.48 | 19.65 | | |
| .708 | ... | 17.40 | ... | 17.01 | 19.26 | ... | ... | ... | ... | ... | 19.40 | | |
| .696 | 16.01 | 17.42 | 17.46 | 17.02 | 19.30 | 18.32 | 19.71 | 19.44 | 19.44 | 19.68 | 19.36 | log ν | 21 |
| .685 | 15.92 | 17.36 | 17.42 | 16.93 | 19.28 | 18.16 | 19.52 | 19.24 | 19.07 | 19.28 | 19.28 | | |
| .674 | 15.93 | 17.16 | 17.31 | 16.79 | 19.15 | 18.12 | 19.49 | 19.14 | 18.92 | 18.96 | 18.99 | .950 | 21.41 |
| .663 | 15.86 | 17.15 | 17.26 | 16.68 | 19.03 | 18.10 | 19.39 | 19.12 | 18.74 | 18.83 | 18.71 | .930 | 21.59 |
| .652 | 15.91 | 17.18 | 17.18 | 16.54 | 19.08 | 18.08 | 19.45 | 19.13 | 18.83 | 18.62 | 18.68 | .911 | * |
| .642 | 15.82 | 17.13 | 17.17 | 16.74 | 18.93 | 18.03 | 19.33 | 19.17 | 18.73 | 18.86 | 18.58 | .892 | 22.01 |
| .632 | 15.75 | ... | 17.06 | 16.81 | 18.85 | 17.92 | 19.43 | 18.95 | 18.66 | 19.05 | 18.43 | .875 | 22.16 |
| .622 | 15.71 | 16.93 | 17.05 | 16.56 | 18.79 | 17.83 | 19.32 | 18.96 | 18.87 | 18.98 | 18.36 | .858 | * |
| .612 | 15.67 | 16.93 | 16.96 | 16.64 | 18.70 | 17.74 | 19.13 | 18.76 | 18.42 | 18.85 | 18.26 | .841 | 21.13 |
| .603 | 15.65 | 16.93 | 16.91 | 16.47 | 18.69 | 17.78 | 19.13 | 18.87 | 18.33 | 18.71 | 18.41 | .825 | 21.39 |
| .594 | 15.74 | ... | 16.97 | 16.46 | ... | 17.67 | 19.05 | 18.78 | 18.21 | 18.64 | ... | .810 | 21.40 |
| .585 | 15.57 | 16.84 | 16.84 | 16.38 | 18.62 | 17.60 | 18.97 | 18.73 | 18.29 | 18.54 | 18.19 | .795 | 21.05 |
| .576 | 15.45 | 16.80 | 16.82 | 16.32 | 18.61 | 17.66 | 18.96 | 18.74 | 18.26 | 18.53 | 18.31 | .781 | 21.38 |
| .567 | 15.37 | 16.74 | 16.83 | 16.23 | 18.56 | 17.42 | 18.82 | 18.53 | 18.20 | 18.56 | 18.06 | .767 | 20.95 |
| .559 | 15.29 | 16.69 | 16.74 | 16.32 | 18.63 | 17.62 | 18.78 | 18.33 | 18.14 | 18.23 | 18.10 | .754 | 20.38 |
| .551 | 15.34 | 16.81 | 16.75 | 16.29 | 18.50 | 17.52 | 18.39 | 18.58 | 18.02 | 18.50 | 18.00 | .741 | 20.15 |
| .542 | 15.32 | 16.66 | 16.50 | 16.16 | 18.20 | 17.46 | 18.89 | 18.37 | 17.92 | 18.26 | 17.94 | .729 | 20.25 |
| .534 | 15.26 | 16.73 | 16.64 | 16.15 | 18.37 | 17.45 | 18.26 | 18.13 | 17.98 | 18.29 | 17.70 | .718 | 20.23 |
| .527 | 15.27 | 16.58 | 16.70 | 16.06 | 18.52 | 17.40 | 18.50 | 18.14 | 17.81 | 18.34 | 17.83 | .691 | 19.43 |
| .519 | 15.27 | 16.66 | 16.68 | 16.11 | 17.91 | 17.18 | 18.53 | 18.31 | 17.99 | 18.26 | 17.85 | .667 | 19.23 |
| .511 | 15.15 | 16.55 | 16.56 | 15.79 | 18.23 | 17.31 | 18.81 | 18.38 | 17.99 | 18.21 | 17.72 | .643 | 19.29 |
| .504 | ... | ... | 16.61 | 16.69 | ... | 16.90 | * | 17.36 | ... | 17.84 | ... | .621 | 19.04 |
| .497 | 14.88 | 16.36 | 16.40 | 15.73 | 18.70 | 17.21 | 18.61 | 18.28 | 18.02 | 18.52 | 17.19 | .599 | 18.87 |
| .489 | 14.97 | 16.26 | 16.56 | 16.03 | 18.17 | 17.45 | 18.89 | 18.22 | 17.68 | 18.24 | 17.21 | .579 | 18.85 |
| .482 | 14.95 | 16.65 | 16.40 | 17.50 | 18.21 | 16.99 | 18.24 | 17.80 | 17.72 | 18.50 | 17.32 | .560 | 18.64 |
| .475 | 14.91 | 16.34 | 16.31 | 16.29 | 17.89 | 17.18 | 19.06 | 17.92 | 17.90 | 17.93 | 17.50 | .541 | 19.33 |
| .468 | 14.97 | 16.38 | 16.72 | 15.60 | 17.92 | 16.90 | 17.94 | 17.81 | 17.60 | 17.72 | 17.37 | .523 | 18.30 |
| .462 | 14.88 | 16.36 | 16.38 | 15.81 | 18.65 | 17.50 | 17.64 | 18.23 | 17.66 | 17.99 | 17.58 | .506 | 18.31 |
| .455 | 14.90 | 16.10 | 16.21 | 15.67 | * | 16.81 | 17.98 | 17.88 | ... | ... | 16.91 | .490 | 18.12 |
| .448 | 14.70 | 16.40 | 16.70 | ... | 17.42 | 17.67 | 18.45 | 17.65 | ... | ... | 17.40 | .474 | 18.83 |
| | | | | | | | | | | | | .459 | 18.30 |

TABLE 4

Hydra Cluster Energy Distribution AB

| log ν | 6 | log ν | 6 | log ν | 6 |
|---|---|---|---|---|---|
| 14.879 | 19.63 | 14.748 | 17.81 | 14.589 | 16.75 |
| .875 | 19.46 | .745 | 17.81 | .585 | 16.68 |
| .871 | 19.39 | .741 | 17.74 | .580 | 16.75 |
| .866 | 19.87 | .738 | 17.66 | .576 | 16.84 |
| .862 | 19.16 | .735 | 17.68 | .572 | 16.71 |
| .858 | 19.72 | .732 | 17.47 | .567 | 16.64 |
| .854 | 19.76 | .729 | 17.86 | .563 | 16.54 |
| .850 | 19.49 | .726 | 17.57 | .559 | 16.68 |
| .846 | 19.60 | .723 | 17.53 | .555 | 16.63 |
| .842 | 19.28 | .720 | 17.54 | .551 | 16.45 |
| .838 | 19.39 | .717 | 17.51 | .547 | 16.48 |
| .834 | 19.64 | .714 | 17.47 | .542 | 16.54 |
| .830 | 19.24 | .708 | 17.54 | .538 | 16.49 |
| .826 | 19.27 | .702 | 17.39 | .534 | 16.51 |
| .822 | 19.23 | .696 | 17.42 | .531 | 16.37 |
| .818 | 19.31 | .690 | 17.37 | .527 | 16.24 |
| .814 | 19.19 | .685 | 17.37 | .523 | 16.41 |
| .810 | 19.14 | .679 | 17.33 | .519 | 16.21 |
| .807 | 18.95 | .674 | 17.27 | .515 | 16.49 |
| .803 | 18.98 | .668 | 17.23 | .511 | 16.42 |
| .799 | 18.56 | .663 | 17.15 | .508 | 16.11 |
| .796 | 18.66 | .657 | 17.15 | .504 | 16.17 |
| .792 | 18.47 | .652 | 17.10 | .500 | ... |
| .789 | 18.40 | .647 | 17.15 | .497 | 16.22 |
| .785 | 18.32 | .642 | 17.06 | .493 | 16.13 |
| .782 | 18.28 | .637 | 17.02 | .489 | 16.21 |
| .778 | 18.28 | .632 | 16.90 | .486 | 16.29 |
| .775 | 18.18 | .627 | 17.04 | .482 | 16.61 |
| .771 | 18.20 | .622 | 16.96 | .479 | 15.88 |
| .768 | 18.28 | .617 | 16.95 | .475 | 16.12 |
| .764 | 18.21 | .612 | 16.84 | .472 | 16.24 |
| .761 | 18.19 | .608 | 16.84 | | |
| .758 | 18.04 | .603 | 16.86 | | |
| .754 | 17.96 | .598 | 16.91 | | |
| .751 | 17.91 | .594 | 16.71 | | |

There are no other redshifts in the present sample as large as that for 3C 295; we shall explore the reasons for this later in the paper.

The brightest galaxy, and occasionally the second or third brightest in each cluster, was observed with the multichannel spectrometer on the 200-inch (5-m) telescope. Bandpasses in most cases were 80 Å for $\lambda < 5800$ Å, and 160 Å for $\lambda > 5800$ Å; in two cases bandpasses of 160 and 360 Å were used. Bandpasses of 40 and 80 Å were employed for the Hydra cluster observations. Observations were made in such a way that all measured bands were contiguous. Integrations were always made in pairs with the galaxy first in one aperture, then in the other, with integration times typically of 600 s. Unless adverse effects such as clouds or deteriorating seeing occurred, individual observations were combined with weights proportional to the integration times. Standard deviations were calculated using Poisson statistics and the photon counts; negative counts were handled in a proper statistical manner.

All observations were made under conditions of moderately good seeing, i.e., stellar image diameters of 1".5 or less. The aperture diameter in arc seconds is given for each object observed in table 1.

The final absolute fluxes $f_\nu$ (ergs $s^{-1}$ $cm^{-2}$ $Hz^{-1}$), given in the form $AB = -2.5 \log f_\nu - 48.60$, are listed in tables 2, 3, and 4 along with the observed frequencies in terms of $\log \nu$. The two objects observed with the 160 and 360 Å bandpasses are listed in the last two columns of table 3, while all the Hydra cluster observations are in table 4. The absolute fluxes are based on the calibration of $\alpha$ Lyrae given by Oke and Schild (1970). In the tables ... means that a measurement was not made or the measurement uncertainty was very large. An asterisk means that the net count was negative. The approximate visual magnitude $V$ can be determined directly by averaging several values of AB in the neighborhood of $\log \nu = 14.740$. Average standard deviations are listed in table 5, where the fractional error in parentheses is applicable between the adjacent values of $\log \nu$. Standard deviations for individual points are occasionally larger than those tabulated, as for example in the case of measurements which include the [O I] λ5577 nightsky line.

Data for the nearby clusters of galaxies which are listed in the top part of table 1 are discussed in the next section.

## III. ANALYSIS OF OBSERVATIONS

### a) *The Magnitude System and Reddening Corrections*

One advantage of spectrophotometry over broad-band photometry in the study of galaxies at large redshifts is that "$K$-corrections" (Sandage 1961*a*) can be avoided entirely by using monochromatic magnitudes at some standard rest frequency. We have chosen

$$\mathrm{VM} = -2.5 \log g_{(\nu_0/1+z)}, \qquad (1)$$

where $\log \nu_0 = 14.740$, $\lambda_0 = c/\nu_0 = 5456$ Å, and $g_\nu$ is the flux in ergs $cm^{-2}$ $s^{-1}$ $Hz^{-1}$ corrected to outside the Galaxy. To relate $g_\nu$ to $f_\nu$ we have adopted the reddening-free polar cap model of Sandage (1972*a*) for the latitude dependence and the relation of Whitford (1958) for the color dependence of the reddening. Note that VM is a monochromatic magnitude, i.e., a logarithm of flux received per unit *observed* frequency, so one must use slightly different cosmological relations from the usual ones which are written in terms of bolometric flux.

The procedure for determining VM is simple: The scan of a distant galaxy is fitted to a standard energy distribution, in this case a high-resolution scan of NGC 4889, to obtain a redshift if one is not known from other data; this determination is usually accurate to about $\pm 0.01$ in $z$. Examples of such fitting are given by Oke (1971). The region from $\log \nu =$ 14.64 to 14.84 in the rest frame of the galaxy is then fitted vertically to obtain VM.

### b) *Aperture Corrections and Standard Diameter*

The aperture corrections are crucial to the use of this photometry for cosmological tests, since the brightness of these galaxies is a strong function of the aperture diameter, and the physical diameter corresponding to a given angular diameter is in turn dependent on the cosmological model. We have chosen to define the magnitude as that corresponding to a fixed physical diameter in the Einstein–de Sitter

TABLE 5

AVERAGE FRACTIONAL STANDARD DEVIATIONS (*parentheses*) BETWEEN VALUES OF LOG $\nu$

| Obj. No. | Log ν (Fractional Standard Deviation) | | | | | | | | | | | | | |
|---|---|---|---|---|---|---|---|---|---|---|---|---|---|---|
| 1 | 14.945 | (0.15) | 14.916 | (0.04) | 14.854 | (0.02) | 14.559 | (0.04) | 14.511 | (0.08) | 14.448 | | | |
| 2 | 14.956 | (0.20) | 14.935 | (0.10) | 14.897 | (0.02) | 14.585 | (0.10) | 14.511 | (0.15) | 14.475 | (0.30) | 14.448 | |
| 3 | 14.956 | (1.00) | 14.916 | (0.10) | 14.862 | (0.05) | 14.822 | (0.02) | 14.576 | (0.08) | 14.511 | (0.15) | 14.475 | (0.30) 14.448 |
| 4 | 14.964 | (1.00) | 14.895 | (0.60) | 14.844 | (0.15) | 14.737 | (0.10) | 14.583 | (0.40) | 14.517 | (0.50) | 14.453 | |
| 5 | 14.906 | (0.25) | 14.871 | (0.15) | 14.807 | (0.05) | 14.567 | (0.10) | 14.511 | (0.30) | 14.455 | | | |
| 6 | 14.879 | (0.25) | 14.850 | (0.20) | 14.834 | (0.10) | 14.803 | (0.04) | 14.563 | (0.09) | 14.511 | (0.15) | 14.472 | |
| 7 | 14.904 | (0.40) | 14.877 | (0.15) | 14.797 | (0.05) | 14.682 | (0.03) | 14.610 | (0.05) | 14.565 | (0.15) | 14.474 | (0.25) 14.453 |
| 8 | 14.945 | (0.50) | 14.879 | (0.15) | 14.799 | (0.10) | 14.559 | (0.25) | 14.475 | (0.50) | 14.448 | | | |
| 9 | 14.923 | (0.40) | 14.877 | (0.15) | 14.763 | (0.06) | 14.574 | (0.20) | 14.488 | (0.35) | 14.460 | | | |
| 10 | 14.913 | (0.25) | 14.868 | (0.15) | 14.860 | (0.10) | 14.790 | (0.05) | 14.565 | (0.14) | 14.474 | (0.20) | 14.453 | |
| 11 | 14.877 | (0.35) | 14.812 | (0.07) | 14.601 | (0.10) | 14.565 | (0.20) | 14.467 | (0.40) | 14.453 | | | |
| 12 | 14.964 | (0.30) | 14.886 | (0.12) | 14.820 | (0.06) | 14.574 | (0.20) | 14.473 | (0.70) | 14.460 | | | |
| 13 | 14.964 | (0.80) | 14.943 | (0.20) | 14.805 | (0.10) | 14.736 | (0.06) | 14.573 | (0.15) | 14.454 | | | |
| 14 | 14.896 | (0.35) | 14.828 | (0.20) | 14.763 | (0.15) | 14.730 | (0.06) | 14.574 | (0.30) | 14.480 | (0.60) | 14.460 | |
| 15 | 14.879 | (0.50) | 14.862 | (0.14) | 14.792 | (0.05) | 14.567 | (0.14) | 14.511 | (0.20) | 14.448 | | | |
| 16 | 14.877 | (0.60) | 14.843 | (0.30) | 14.776 | (0.08) | 14.549 | (0.30) | 14.460 | | | | | |
| 17 | 14.877 | (0.80) | 14.860 | (0.15) | 14.730 | (0.07) | 14.565 | (0.15) | 14.473 | (0.25) | 14.453 | | | |
| 18 | 14.964 | (0.25) | 14.895 | (0.15) | 14.852 | (0.07) | 14.540 | (0.25) | 14.473 | (0.40) | 14.447 | | | |
| 19 | 14.877 | (0.30) | 14.820 | (0.15) | 14.756 | (0.10) | 14.601 | (0.15) | 14.517 | (0.35) | 14.453 | | | |
| 20 | 14.964 | (0.80) | 14.913 | (0.25) | 14.868 | (0.10) | 14.763 | (0.07) | 14.574 | (0.10) | 14.495 | (0.25) | 14.453 | |
| 21 | 14.950 | (0.70) | 14.858 | (0.25) | 14.767 | (0.10) | 14.579 | (0.30) | 14.459 | | | | | |
| 22 | 14.933 | (0.50) | 14.886 | (0.15) | 14.565 | (0.30) | 14.474 | (0.80) | 14.467 | | | | | |
| 23 | 14.897 | (0.70) | 14.879 | (0.25) | 14.764 | (0.08) | 14.576 | (0.20) | 14.497 | (0.30) | 14.448 | | | |
| 24 | 14.879 | (0.50) | 14.814 | (0.25) | 14.792 | (0.10) | 14.714 | (0.06) | 14.594 | (0.20) | 14.482 | (0.60) | 14.448 | |
| 25 | 14.877 | (0.50) | 14.820 | (0.25) | 14.737 | (0.10) | 14.574 | (0.30) | 14.460 | | | | | |
| 26 | 14.879 | (0.45) | 14.845 | (0.20) | 14.751 | (0.10) | 14.559 | (0.15) | 14.497 | (0.35) | 14.462 | | | |
| 27 | 14.871 | (0.45) | 14.830 | (0.15) | 14.771 | (0.10) | 14.567 | (0.25) | 14.497 | (0.30) | 14.462 | | | |
| 28 | 14.879 | (0.25) | 14.799 | (0.10) | 14.714 | (0.04) | 14.551 | (0.20) | 14.527 | (0.15) | 14.462 | (0.70) | 14.448 | |

(Friedmann zero-pressure, zero cosmological constant, $q_0 = \frac{1}{2}$) model. The variation of this diameter with $q_0$ can then be incorporated explicitly into the cosmological relation, as we shall see. The diameter chosen is 32 kpc for $c/H_0 = 5000$ Mpc, or $H_0 \sim 60$ km s$^{-1}$ Mpc$^{-1}$. The (diaphragm diameter, redshift)-relation is then (see, for example, Weinberg 1972, p. 485),

$$\gamma = 1.320 \frac{1 + z}{2[1 - (1 + z)^{-1/2}]} \text{ arcseconds} . \quad (2)$$

This standard diameter is close to that chosen by Peterson (1970), who used 33.3 kpc for our value of $H_0$. Corrections to the standard diameter were done by interpolation wherever possible, and by the use of a standard growth curve when not. The corrections are never very large, and we have adopted a power-law approximation to the growth curve for the projected luminosity $L$ within angular radius $\gamma$,

$$L \propto \gamma^{\alpha} , \quad (3)$$

over the region of interest. The exponent $\alpha$ is about 0.6 for Sandage's growth curve (Sandage 1972*a*) and 0.8 for Peterson's, and the average for our data is 0.72. We have adopted $\alpha = 0.7$, but the results are not very sensitive to the choice. We shall later use relation (3) to construct the redshift-magnitude diagram; it is important here only to note that it need hold only in the neighborhood of the standard diameter, since the differences in angular diameter from that in the $q_0 = \frac{1}{2}$ model are at most 30 percent even at $z = 1$ for the range $0 \leq q_0 \leq 2$. The power-law approximation is excellent over such a small range, and the technique stands or falls only on the question of whether the use of *any* standard growth curve is justified; Sandage (1972*a*) has investigated this question in some detail.

Sandage has chosen a much larger standard diameter than we use, and the reasons for our choice should perhaps be discussed. There is first the question of optimal signal-to-noise. It can easily be shown that if $\alpha = 1$, and the sky signal dominates the total count, the signal-to-noise ratio for a chopping pulse-counting detector such as the multi-channel spectrophotometer is independent of diaphragm diameter, since both the flux and the photon shot noise from the sky grow linearly with the diaphragm diameter. There is a region at smaller diameters where $\alpha \sim 1$; and for an ideal, noiseless machine in the absence of seeing, one should work there for optimal signal-to-noise. In the real world, however, one must contend with both dark noise in photomultipliers and seeing, and the slightly larger diameters used above represent a reasonable compromise in these regards. The aperture is 5″.4 even for $z = 0.5$, which is safely out of seeing difficulty in good seeing, and is large enough that dark noise in the present instrument is not too important.

A rather more important criterion concerns the galaxies themselves, and the sense in which they are standard candles. Do the brightest cluster galaxies exhibit standard luminosities independent of the measuring aperture, or is the dispersion minimized for some chosen aperture size? We unfortunately do not have sufficient data to answer that question; we shall see that our dispersion is bigger than that obtained by Sandage, but we choose not to make some of the corrections and exclusions which he makes, and the case remains unclear. It is clear that corrections for the presence of faint cluster members in the diaphragm are minimized for small diaphragms; it is our feeling that such detailed corrections cannot be reliably made for faint, distant clusters, and so we choose not to make them at all for any of the data. *Thus our magnitudes are for all of the light in a circle of 16 kiloparsecs projected radius centered on the brightest cluster member.* We also do not exclude or treat as special the objects which Morgan and Lesh (1965) classify as cD galaxies (for reasons discussed below, we *do* choose not to incorporate a set of data for objects of this type of intermediate redshift in our analyses for $q_0$ for cogent reasons of completeness and sampling correctness). This again is not because we believe they are not different from ordinary giant ellipticals—they clearly are—but simply because we do not believe they can reliably be recognized at very large redshifts. All of these efforts are to reduce any bias which would occur if the bright and faint parts of the sample were treated in a subtly different fashion. The present level of sensitivity and accuracy is such that bias of this type may well dominate the error.

The physical radius in kpc ($q_0 = \frac{1}{2}$, $H_0 = 60$ km s$^{-1}$ Mpc$^{-1}$) corresponding to the aperture used for the observations and the aperture correction in magnitudes are given in table 1. By applying the reddening correction and aperture correction to the values of VM, the intrinsic magnitudes $V_I$ are derived. These are also tabulated in table 1, as are the values of log $z$ and $z$.

### c) *Analysis of Nearby Clusters*

While the multichannel spectrometer techniques described in § II work very well for large-redshift galaxies, it is not possible to extend them directly to flux measurements of nearby galaxies, because the largest unvignetted aperture available in the instrument is only 14″ in diameter. It has thus been necessary for the bright end of the Hubble diagram to rely on previous broad-band photometry and to relate it directly to the spectrophotometric system. We have chosen a mixture of photometry by Peterson (1970) and by Sandage (1972*a*, 1973*a*) for a selection of nearby clusters of galaxies, which are selected from catalogs of Humason *et al.* (1956), Abell (1958), and Sandage (1972*a*). The list of these clusters is given in the top half of table 1. In the first column, labeled "code," S stands for photometry by Sandage, P for photometry by Peterson. The only difference between the top half of the table 1 and the lower half is in the measurement of the magnitudes. In the case of the nearby clusters, we must rely on the visual magnitude $V$ itself. To derive VM from $V$ one must use a relation of the form

$$\mathrm{VM} = V - K(z) - 2.5 \log (1 + z) + C ; \quad (4)$$

we have used the $K$-corrections $K(z)$ of Schild and Oke (1971); the adopted zero points are $C = +0.01$ for the Peterson data and $C = -0.09$ for the Sandage data. Direct intercomparison of the Peterson and Sandage data, where possible, shows a standard deviation of the difference of the magnitudes for a given object as 0.08, with a zero-point difference of $0.10 \pm 0.03$ (s.d.). The zero-point correction from Sandage's data to our VM system is found by comparing small diaphragm measurements for a number of bright galaxies for which MCSP observations exist from other programs, and is quite well determined, with a standard deviation of about 0.03. These uncertainties are all very much smaller than the standard deviation in the luminosity function of brightest cluster members, but so are the effects we are looking for, so extreme care must be exercised.

As in the lower part of table 1, once VM has been calculated by equation (4), using the appropriate $K$-correction listed in the table, then application of the reddening and aperture corrections yields the intrinsic magnitude $V_I$ listed in the table.

## IV. CONSTRUCTION OF THE HUBBLE DIAGRAM

In a Friedmann cosmology in which the metric is

$$ds^2 = c^2 dt^2 - R^2(t)[du^2 + \sigma^2(u)(d\theta^2 + \sin^2 \theta d\phi^2)] , \quad (5)$$

the monochromatic flux $F_\nu$ from a source of luminosity $L_\nu$ at coordinate distance $u$ is

$$F_\nu = \frac{L_{\nu(1+z)}}{4\pi R_0^2 \sigma^2(u)(1 + z)} , \quad (6)$$

where, of course, $R_0$ is the present scale factor, and $(1 + z) = R_0/R(\tau_0)$, where $\tau_0$ is the epoch of emission (see, for example, Weinberg 1972, ch. 14, 15). For the case in which the pressure and the cosmological constant both vanish, the model is uniquely specified by $H_0$, the present Hubble constant, and $q_0$, the deceleration parameter, which satisfy

$$H_0 = R_{,t} R^{-1})_0 ,$$

$$q_0 = -\frac{R_{,tt} R}{R_{,t}^2}\Big)_0 = \frac{4\pi G \rho_0}{3 H_0^2} , \quad (7)$$

where $\rho_0$ is the present mean matter density. The coordinates can be chosen, and conventionally are, such that the scale factor $R$ is proportional to $c/H_0$, the Hubble distance, and the quantity $\sigma(u)$ is dimensionless and a function only of $q_0$ and $z$. Let

$$\mathscr{Z}_q(z) = H_0 R_0 \sigma_{q_0}[u(z, q_0)] c^{-1} , \quad (8)$$

where $\mathscr{Z}_q \sim z$ for small $z$ for any $q_0$, and is a

dimensionless measure of the luminosity distance. Then (Weinberg 1972, p. 485)

$$\mathscr{Z}_q(z) = \frac{q_0 z + (q_0 - 1)[(1 + 2q_0 z)^{1/2} - 1]}{q_0^2(1 + z)}, \quad (9)$$

and

$$F_\nu = \frac{H_0^2 L_{\nu(1+z)}}{4\pi c^2 \mathscr{Z}_q^2(z)(1 + z)}. \quad (10)$$

Suppose $L_\nu$ is a power law in the projected diaphragm radius, $L_\nu = L_{0\nu}(r/r_0)^\alpha$. We observe (or correct to) an angular diaphragm radius which, *if* $q_0$ *were* $\frac{1}{2}$, would project into a standard distance $r_0 = 16$ kpc at the redshift of the source. Thus the diaphragm radius $\gamma$ is

$$\gamma = \frac{r_0}{[R\sigma(u)]_{q=1/2}} = \frac{H_0 r_0(1 + z)}{c\mathscr{Z}_{1/2}(z)}, \quad (11)$$

the real projected radius is

$$r = R\sigma_q(u)\gamma = r_0 \frac{\mathscr{Z}_q(z)}{\mathscr{Z}_{1/2}(z)}, \quad (12)$$

and the luminosity within the projected radius is

$$L_\nu = L_{0\nu}[\mathscr{Z}_q(z)/\mathscr{Z}_{1/2}(z)]^\alpha. \quad (13)$$

Thus the observed flux is

$$F_\nu = \frac{H_0^2 L_{0\nu(1+z)}}{4\pi c^2(1 + z)\mathscr{Z}_q^{2-\alpha}(z)\mathscr{Z}_{1/2}^\alpha(z)}, \quad (14)$$

where now $L_{0\nu}$ is independent of $q_0$ and (except for possible evolutionary effects) $z$ for a given kind of galaxy. With the power-law assumption for the growth curve in the neighborhood of $\gamma_0$, then, we can plot a Hubble diagram in which the aperture corrections are already incorporated. *Note that the net effect of the aperture corrections is to decrease the sensitivity of the flux to* $q_0$, *since the dependence goes from* $\mathscr{Z}_q^{-2}$ *to* $\mathscr{Z}_q^{-2+\alpha}$. *This decrease in sensitivity is fundamental, and it matters not in the slightest whether the aperture effect is explicitly allowed for, or iterated for, or otherwise treated, so long as a standard metric diameter is used to define the luminosity.* That this must be so is most easily seen by consideration of a "galaxy" of uniform surface brightness, for which $\alpha = 2$; since observed surface brightness does not depend on $q_0$, no amount of cleverness will extract $q_0$ from surface brightness measurements, and the larger $\alpha$ (in $0 \leq \alpha < 2$), the nearer the galaxy becomes a uniform surface-brightness source. This sensitivity decrease is primarily important in that it increases the estimated errors in the conventional fitting techniques by roughly the factor $2/(2 - \alpha)$.

The next point is more difficult. The brightest cluster galaxies are not exactly standard candles, of course, but have a dispersion in absolute magnitude, which may be as small as 0.25 mag, if careful selection and corrections are made (Sandage 1972*a*), and is about 0.4 mag if they are not. The total separation of $q_0 = 0$ from $q_0 = 2$ in the "aperture-corrected" Hubble diagram at $z = 0.4$ is only 0.5 mag; that between $q_0 = 0$ and $q_0 = \frac{1}{2}$ is only 0.18 mag. It is thus clear that sampling differences along the diagram can play havoc with any analysis, since the effects we seek are small compared with the intrinsic dispersion in the data.

We seek a criterion by which objects are selected, which can be related to a variable which we can use as the independent (sampling) variable in the Hubble diagram. Previous analyses have used the redshift; the redshift is appealing, because the distribution of apparent magnitude at a given redshift is independent of $K$-corrections and cosmology, and is the same as the distribution of absolute magnitudes in a given volume of space—*if* the sampling at a given redshift is in some sense complete or at least unbiased. It is painfully clear, however, that it is neither complete nor unbiased at any but the very smallest redshifts. Consider, as an extreme example, 3C 295, at $z = 0.46$. It lies well above the mean absolute magnitude in any fit; to have a complete sample at this redshift would require redshifts for objects at least a magnitude fainter, and no redshifts for objects this faint exist. Thus there is no chance for the construction of an unbiased sample at large redshift as long as magnitude limits exist.

This state of affairs forces us to abandon the use of redshift as the sampling variable. It is clear that the apparent magnitude is much better in this respect. In general, clusters are found in a survey because the brightness of their members—in the wavelength range in which the survey is conducted—lies within some range; there is no selection on redshift, only on brightness. One cannot use $V_I$ or $V - K(z)$ or other "$K$-corrected" magnitudes either. One must use $V$, if the surveys were performed on $V$ plates; nature then does the selection in redshift, and provided one can derive the redshift distribution at a given $V$, the statistical problem of fitting a curve on the $(V, z)$-plane is well posed.

The real situation is not so clear-cut as this, of course, because the sample is not the result of a homogeneous survey. The inclusion of 1447+2617 and 0024+1654 is probably justifiable, since they would have been included in the 48-inch sample if they had been in the right part of the sky, and were found in any case by accident. The case of 3C 295 is shakier, since it was pointed to by another indicator, namely, its intense radio emission. It does fall within the magnitude limits of the 48-inch survey, but it is so much brighter than the other cluster members that it is slightly doubtful that the cluster would have been recognized in the survey. Even with these questions aside, it must be shown that the existence of a very powerful radio source, which makes distant objects like 3C 295 show up in the 3C, does not bias the optical brightness of the parent galaxy—note that it is *not* enough to show that radio galaxies are distributed in magnitude like brightest cluster galaxies, which Sandage (1972*b*) has done; one must show that the optical brightness (and hence probably the mass) is

uncorrelated with radio power. The complications are severe enough that we prefer not to use galaxies selected on their radio properties at all. In our analysis, we will quote results with 3C 295 left in and taken out, and leave the reader to make his own judgments—the fact that it is such an extreme object only complicates the psychology of its treatment.

Let us now discuss the construction of the Hubble diagram which we will use in an analysis. We will use a magnitude $S$ which is approximately $V$ for the abscissa, since the sampling band is approximately the $V$ band, and the sample is contaminated by material which was found on $V$ plates. Since we have gone to great pains to rid ourselves of the $K$-correction problem by doing spectrophotometry, this may seem a regression, but it is in fact not; we use the $K$-correction only to make mathematical transformations, which transform data and theory alike. *The accuracy of the adopted K-correction is irrelevant* except for its effect on the statistics; if there were no dispersion in magnitude, an arbitrarily incorrect one would still yield the correct answer. The plot in $V_I$, $\log z$ is approximately linear (fig. 2), over a large range in $q_0$, but this is not the case for the use of $S$ as abscissa plotted against $\log z$. We will see later that this approximate linearity is rather useful in the statistical treatment; we therefore choose to use a different function of $z$ than the logarithm for the ordinate. It is convenient to make the relation for a standard candle strictly linear for some $q_0$; and since $q_0 = \frac{1}{2}$ has been used as the "fiducial" value in the diameter discussion, we use it here too. We define

$$\zeta = 5 \log [(1 + z)\mathscr{L}_{1/2}(z)] + k_s(z)$$
$$S = 2.5 \log (1 + z) + V_I + k_s(z); \qquad (15)$$

we will usually simply call the quantity $\zeta$ the "distance"; it is exactly the distance *modulus* to within an additive constant for the magnitude $S$ and $q_0 = \frac{1}{2}$. Appeal to equation (14) shows that for a standard candle and $q_0 = \frac{1}{2}$,

$$S = \mu + \zeta, \qquad (16)$$

and

$$\mu = M_{V_I} + 5 \log (c/H_0) - 5,$$

where $M_{V_I}$ is the absolute monochromatic magnitude at $\log \nu_0 = 14.740$. We call $\mu$ the *reduced absolute magnitude* (RAM). It is essentially the same quantity as Sandage's (1972*a*) C. All dependence on the Hubble constant is swallowed in the definition of $\mu$.

The function $k_s(z)$ is a smoothed version of the $K$-correction as obtained by Schild and Oke; we used the interpolation formula

$$k_s(z) = 0.918 \tan^{-1} [5.20(z - 0.340)] + 0.970, \qquad (17)$$

which is analytic and represents $K_V$ to within $\pm 0.06$ mag in the range $0 \leq z \leq 0.6$. Note that any uncertainty in $k_s$ does not make itself felt in the Hubble diagram; the relation (16) and similar ones for other $q_0$ do not depend on $k$. The correction serves only to transform the magnitudes into suitable sampling values.

For other values of $q_0$ equation (16) becomes

$$S = \mu + \zeta + 2.5(2 - \alpha) \log [\mathscr{L}_q(z)/\mathscr{L}_{1/2}(z)], \qquad (18)$$
$$\equiv \mu + f_q(\zeta),$$

where $z$ is now a function of $\zeta$ through equation (17). The data and a set of theoretical curves are plotted in the $(S, \zeta)$-plane in figure 3.

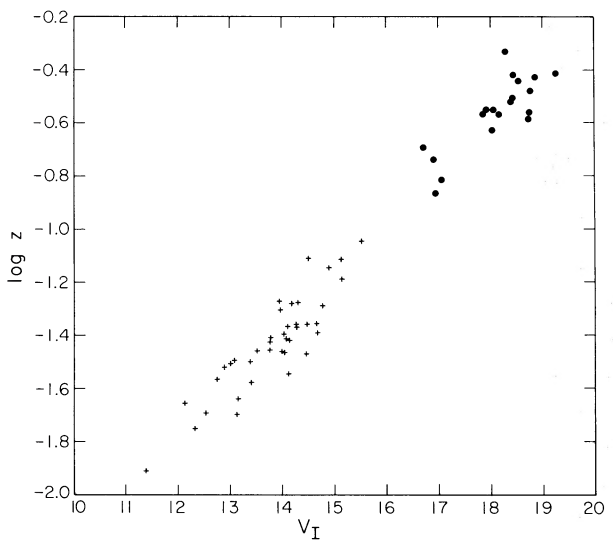


FIG. 2.—The Hubble diagram for the data used in the paper. *Solid dots*, scanner data; *crosses*, broad-band photometric data.

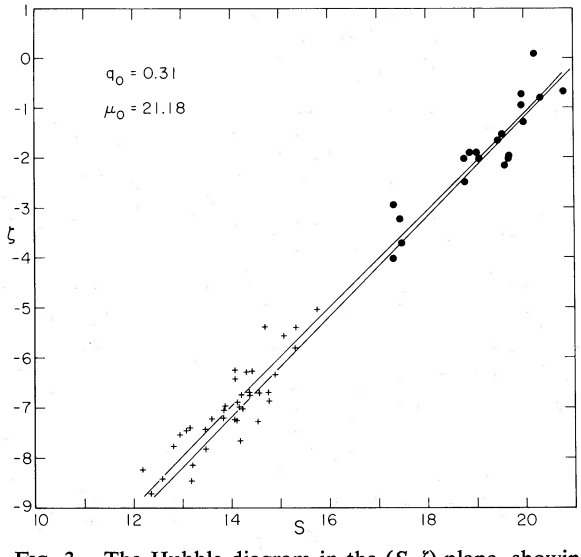


FIG. 3.—The Hubble diagram in the $(S, \zeta)$-plane, showing the fit for the case (3C 295 in, no evolution) (*upper line*). The lower line is the corresponding line with no volume correction, i.e., for $\sigma = 0$. The difference is $\sigma^2 \xi$ for this case.

## V. STATISTICAL ANALYSIS OF THE HUBBLE DIAGRAM

We must now find the distribution function of $\zeta$ at a given $S$, supposing that we know the luminosity function. This problem is well known in a classical context and was solved long ago (Malmquist 1924) under the assumption that the luminosity function is Gaussian. Our problem is complicated by the geometry, but is a straightforward extension of the classical technique.

Suppose that the luminosity function is $\phi(\mu)$; i.e., the expected number of brightest cluster galaxies in a comoving volume element $dV$ (we assume, of course, that the total number of these objects is conserved; that they are not created by magic from quasar effluvia or turn into pumpkins) and range of $RAM\ d\mu$ is

$$\langle dN\rangle = \phi(\mu)d\mu dV = \phi(\mu)\frac{dV}{d\zeta}\,d\mu d\zeta\,. \tag{19}$$

Since $S = \mu + f_q(\zeta)$, we can write

$$\langle dN\rangle = \phi[S - f_q(\zeta)]\frac{dV}{d\zeta}\,dSd\zeta\,. \tag{20}$$

Thus the distribution function for $\zeta$ for a given object at observed magnitude $S$ is

$$\psi(\zeta) = C\phi[S - f_q(\zeta)]\frac{dV}{d\zeta}\,, \tag{21}$$

Where $C$ is a constant chosen to make the integral of $\psi$ unity. Let $\mu_0$ be the mean absolute magnitude for a sample selected in a volume of space, i.e.,

$$\mu_0 = \frac{\int \mu\phi(\mu)d\mu}{\int \phi(\mu)du}\,. \tag{22}$$

Now we have been very careful to set up the problem so that $f_q(\zeta)$ is nearly linear in $\zeta$ [recall that $f_{1/2}(\zeta) \equiv \zeta$], and in fact has nearly unit slope. We also know from Sandage's work that the standard deviation $\sigma$ in the absolute magnitudes is small, so that, for example, the quantity $dV/d\zeta$ changes in an approximately linear fashion over a range of $\zeta$ of order $2\,\sigma$. Then the mean $\zeta$ for a sample observed at $S$ is given by

$$\begin{aligned}\langle\zeta\rangle &= C\int \zeta\phi(S - f_q(\zeta))\frac{dV}{d\zeta}\,d\zeta \\ &= C\int \zeta\phi(S - f_q)\frac{dV}{df_q}\,df_q\,.\end{aligned} \tag{23}$$

Let $\zeta_*$ be defined such that $S - f_q(\zeta_*) = \mu_0$; i.e., $\zeta_*$ is the distance a source of absolute magnitude $\mu_0$ observed at an apparent magnitude $S$ would have if $q_0 = q$; it is clear that for $\sigma = 0$, $\langle\zeta\rangle$ must be $\zeta_*$. Then if $x = S - f_q(\zeta) - \mu_0$, we can write

$$S \simeq \zeta_* + \frac{d\zeta}{df_{q^*}}\,x \tag{24}$$

with an error, when integrated over $\phi$, which is of the order $\sigma^2 d^2\zeta/df_q^2$, both terms of which are small. Inserting expression (24) into (23), and expanding $dV/df_q$ about $f_{q^*} = S - \mu_0$, we have

$$\langle\zeta\rangle = \zeta_* + C\int x\frac{d\zeta}{df_{q^*}}\phi(x)\left(\frac{dV}{df_{q^*}} + x\frac{d^2V}{df_{q^*}^2}\right)dx\,.$$

The term in $dV/df_{q^*}$ vanishes, and, to order $\sigma^2$, $C(dV/df_{q^*})\int d(x)dx = 1$, so

$$\begin{aligned}\langle\zeta\rangle &= \zeta_* + \frac{d\zeta}{df_q}\frac{d^2V}{df_q^2}\left(\frac{dV}{df_q}\right)^{-1}\Bigg]_*\sigma^2 \\ &\equiv \zeta_* + \xi\sigma^2\,.\end{aligned} \tag{25}$$

It is easy to verify that, classically, where $\zeta = f_q = 5\log r + \text{const.}$ the correction term is the Malmquist expression $0.6\,\sigma^2 \ln 10$.

To the order we are interested in, the dispersion in $\zeta$ would be the same as that in $\mu$ except for the fact that $d\zeta/df_q$ is slightly different from unity. Clearly the standard deviations are related by

$$\text{s.d.}(\zeta) \simeq \frac{d\zeta}{df_q}\,\text{s.d.}(\mu)\,. \tag{26}$$

To evaluate the correction $\xi$ we need the function $dV/df_q$ and its derivative. From the metric (5), we see that the coordinate volume element, normalized to proper volume at the present epoch, is $dV = 4\pi R_0{}^3\sigma^2(u)du$. But along an incoming light ray

$$du = \frac{-cdt}{R(t)}\,,$$

and

$$dz = d(R_0/R) = \frac{-R_0R_{,t}}{R^2}\,dt = -(1 + z)H(z)dt\,.$$

From the Einstein dynamical equations for the metric (5), it follows that

$$H(z) = H_0(1 + z)(1 + 2q_0z)^{1/2}\,.$$

Using the definition of $\mathscr{Z}_{q_0}$, then, we can write with the above results

$$\frac{dV}{dz} = \frac{4\pi C^3}{H_0{}^2}\frac{\mathscr{Z}_q{}^2}{(1 + z)(1 + 2q_0z)^{1/2}}\,. \tag{27}$$

The other derivatives follow from direct differentiation of $dV/dz$, $f_q(z)$, and $\zeta(z)$. The results are messy, but there is no difficulty. Note that such expressions as $dV/df_q$ involve the $z$-derivative of the $K$-correction, and it is for this reason that it is probably more important to have a smooth $K$-correction defining $S$ than an accurate one.

We find

$$\xi = \left(\frac{df_q}{dz}\right)^{-2}\left(\frac{2d\mathscr{Z}_q/dz}{\mathscr{Z}_q} - \frac{1}{1 + z} - \frac{q_0}{1 + 2q_0z} - \frac{d^2f_q/dz^2}{df_q/dz}\right)\frac{d\zeta}{dz}\Bigg]_*\,. \tag{28}$$

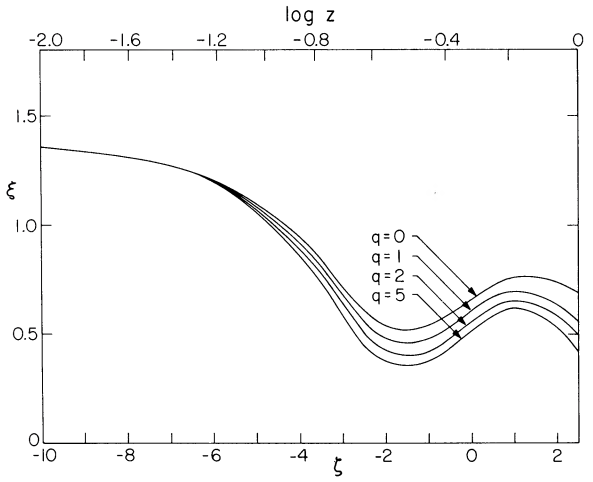


FIG. 4.—The volume correction $\xi$ as a function of $\zeta$ for several values of $q$.

The behavior of $\xi$ is similar for all models; for low redshifts, $\xi \simeq 1.38$, the classical value. As the distance increases, the volume increases more slowly than classically, due both to the geometry and the $K$-correction, so $\xi$ decreases slowly, reaching values around unity for $z = 0.12$, and decreasing to about 0.5 at redshifts about 0.3, after which it changes little to redshifts of unity. The behavior for several values of $q_0$ is plotted in figure 4. Since $\sigma \sim 0.4$, as we shall see, the mean absolute magnitude at a given apparent magnitude differs from the mean in a given volume of space by an amount which varies from about 0.22 mag for nearby objects to about 0.08 at large redshifts.

A valid criterion for the accuracy of the approximation is that $\xi$ change little in an interval $(\zeta - \sigma, \zeta + \sigma)$; the slope is greatest at $\zeta \sim -0.3$, $z \sim 0.2$, where $\xi$ changes by $\sim 0.18$ in an interval of 0.8 in $\zeta$. The error in $\sigma^2\zeta$ is thus bounded by $\sim 0.028$ in this region, but this is a rather pessimistic estimate.

We shall find that the observed distribution of $\zeta$ is normal to within the errors, which corresponds closely to a normal form for $\phi$. In this case, it is well known (see, e.g., Cramér 1958) that the least-squares and maximum-likelihood methods coincide. Maximum-likelihood techniques in general possess the highest efficiency of all fitting schemes, and of course the simplest and best understood of fitting schemes is least squares; it is fortunate that Nature has seen fit to distribute the brightnesses of these objects approximately normally.

Furthermore, our choice of coordinates gives approximately equal weights at all values of $S$, so that the least-squares process is simple. In practice, we form

$$\epsilon = \sum [\zeta_i - \zeta_*(S_i - \mu_0, q_0) - \sigma^2\xi_*(S_i - \mu_0, q_0)]^2 , \tag{29}$$

where $(\zeta_i, S_i)$ are the distance and magnitude of sample point $i$, $\zeta_*$ is, as before, chosen such that $f_q(\zeta_*) = S_i - \mu_0$, and $\xi_*$ is the corresponding volume correction. The method used is to construct tables of $\zeta$, $f_q$, and $\xi$ as functions of $z$ and $q_0$, since we have explicit expressions in terms of these variables. We then interpolate into them at a value of $f_q = S_i - \mu_0$ to find the values of $\zeta_*$ and $\xi_*$. A table of $\epsilon(q_0, \mu_0)$ is thus constructed, and the minimum is found by conventional techniques. The residuals are then analyzed to redetermine $\sigma^2$, since it enters weakly in the volume correction term, and the whole process repeated. We have carried the technique one step further, to redefine $\zeta$ as $f_q$ for the $q$ of the last iteration, but this is evidently an unnecessary refinement.

The variance of the estimates for $q_0$ and $\mu_0$ can be obtained in conventional ways; the expressions are

$$\begin{aligned} \text{var}\,(q_0) &= \sigma^2(D^{-1})_{qq} , \\ \text{var}\,(\mu_0) &= \sigma^2(D^{-1})_{\mu\mu} , \end{aligned} \tag{30}$$

where the matrix $D$ is defined as

$$D_{xy} = \sum_i \frac{\partial g_i}{\partial x}\frac{\partial g_i}{\partial y} , \tag{31}$$

$x, y = \mu_0$ or $q_0$, and $g_i = \zeta_{*i} - \sigma^2\xi_{*i}$. One can easily also find the sensitivity of $q_0$ to errors in $\mu_0$ and vice versa by noting how the minimum in $\epsilon$ considered as a function of $q_0$ moves as one changes $\mu_0$, or vice versa.

## VI. RESULTS FOR NO EVOLUTION

Before we discuss results, we need to make a few remarks about the sample. The low-redshift sample of Peterson is a well-defined, reasonably magnitude-limited sample (the magnitude is Abell's red magnitude, but the $K$-corrections are so small here that no distinction need be made). We exclude part of the middle redshift scanner sample, namely Abell 1961 and 2317, since it violates one selection criterion. These galaxies were measured as part of a program drawn from the list of Morgan and Lesh (1965) of cD systems—and *every one* lies above the mean Hubble line. There can be little doubt that the cD phenomenon is very real, and selection favors the bright end of the brightest cluster galaxy luminosity function. We agreed not to exclude cD's from a random sample, but we must exclude those which were chosen *because* they were cD's. This leaves us with very little redshift data in the vicinity of 0.20, but this hardly matters.

We are left with a sample of 60 or 59, depending on whether we include 3C 295 or not, and we obtain

$$\begin{aligned} q_0 &= 0.31 \pm 0.68\ \text{(s.d.)} \quad (3C\ 295\ \text{in}) , \\ q_0 &= -0.15 \pm 0.57\ \text{(s.d.)} \quad (3C\ 295\ \text{out}) . \end{aligned} \tag{32}$$

Since we obtain values of $q$ which can go negative, it is necessary for the analysis to extend the cosmological models to negative $q_0$, which we do by simple analytic continuation; we simply use the analytic expression for everything with $q_0$ negative. These "models" are not physical, since they correspond to pressureless models with a uniform *negative* energy density; in

particular, $q_0 = -1$ is *not* the steady state, but its optical properties are similar for small redshifts (the curvature index $k = -1$ for all of these models).

It is perhaps appropriate to remark on the comparison of these results with the latest results of Sandage (1972*a*) and Sandage and Hardy (1973) for a sample which contains far fewer high-redshift objects. The formal error of our estimate is similar because of the large standard deviation in our sample (we have discussed why we have chosen to live with this), because of the inclusion of the effect of aperture corrections on the *error*, which Sandage neglects, and because we have demanded that the analysis be done with *magnitude* as the sampling variable. The mean redshift at our magnitude limit of $S \sim 20.2$ is only about 0.35, and the sensitivity of the cosmological effects to $q_0$ is much smaller there than at $z = 0.46$. The bulk of our high-redshift sample is fainter (absolutely) than his; and this, with the effects of incompleteness at large $z$, substantially lower the estimate for $q_0$. There is an equally serious incompleteness, however, in his (and our) low-redshift sample, since the numbers increase nowhere nearly as fast as $\mathscr{L}^3$ where most of the data are. This effect, in fact, more than cancels the effect of the cutoff, since the volume correction and the data density are both large for small $z$. Our analysis is unaffected by the incompleteness so long as there is no redshift bias at a given magnitude. It is clear that one needs a larger faint sample before meaningful statements about $q_0$ can be made—in particular, before the crucial decision of whether $q$ is greater or less than $\frac{1}{2}$ can be commented upon with any confidence. We defer general comments until after we look briefly at evolutionary effects.

## VII. EVOLUTIONARY EFFECTS

The realization that the evolution of the light of elliptical galaxies may play an important role in the determination of $q_0$ is almost as old as serious attempts to use the Hubble diagram technique for the purpose. The crux of whether evolution is important or not hinges on the question of whether the light of elliptical galaxies is dominated at $V$ by red giants or red dwarfs. If the latter, the evolutionary effects are in any case small, and can even be of the sense that galaxies *brighten* as they age, since with such a steep main-sequence luminosity function as is required for dwarfs to dominate the light, more giants are produced per unit time as the system ages, and the giant luminosity is nearly independent of the parent mass (Sandage 1961*b*; Spinrad 1972).

Recent evidence from both continuum colors and infrared spectral features indicate, however, that the light of the systems is probably giant-dominated throughout the visible and near infrared (Tinsley 1973; Whitford 1972; Baldwin *et al.* 1973), and that the slope $x$ of the main sequence mass function, defined as

$$\frac{dN}{dm} = Cm^{-(1+x)} \tag{33}$$

probably does not exceed 2. Tinsley (1972*a*, *b*) has shown that, under quite general conditions,

$$t\frac{dM_V}{dt} = 1.3 - 0.3x \tag{34}$$

for systems between about 4 and 13 billion years old, in which all star formation occurred as a burst at the beginning. Thus,

$$\mu = \mu_0 + (1.3 - 0.3x)\ln(t/t_0)\,.$$

Objects in the past were *brighter*, and we overestimate $q_0$ if we neglect evolution. The time corresponding to a given redshift is

$$t = \frac{q_0}{H_0}\left(\frac{k}{2q_0 - 1}\right)^{3/2} k(S_k^{-1}(y) - y)\,, \tag{35}$$

where $k$ is the curvature index ($+1$ for $q_0 > \frac{1}{2}$, $-1$ for $q_0 < \frac{1}{2}$),

$$y = \left(\frac{2q_0 - 1}{k}\right)^{1/2} \frac{(1 + 2q_0 z)^{1/2}}{q_0(1 + z)}\,, \tag{36}$$

and $S_k(y) = \sin y$ for $k = +1$, $\sinh y$ for $k = -1$.

We included the effects of evolution in an exact (given the form of the evolution) but not quite statistically satisfactory way; we modified each $S_i$ by adding to it a correction

$$\delta S_i = (1.3 + 0.3x)\ln(t/t_i)$$

for a given trial value of $q_0$ (held constant throughout a given least squares solution) to normalize all brightnesses to their present value. This disturbs slightly the position of $S$ as a sampling variable; it would have been better, perhaps, to calculate the mean line with the added effect of evolution, but the differences are slight. We obtain

$$q_0 = -0.43 \pm 0.54 \quad (3C\ 295\ in)\,,$$

$$q_0 = -1.27 \pm 0.62 \quad (3C\ 295\ out)\,,$$

for $x = 2$. These values are in approximate agreement with Tinsley's (1972*a*) estimates for the change in the measured value of $q_0$ introduced by evolution when aperture effects are included. These estimates, and the value of $x$, are of course still subject to considerable controversy, not to mention simple uncertainty.

## VII. COMMENTS AND CONCLUSION

The principal results of the four cases considered (3C 295 in and out, no evolution, and Tinsley evolution with $x = 2$) are presented in table 6. The entries are mostly self-explanatory; $\sigma_{q_0}$ ($\mu_0$ fixed) is the standard deviation in $q_0$ if $\mu_0$ is regarded as determined, $\sigma_\mu$ is the standard deviation of the residual magnitudes about the mean line, and $dq_0/d\mu_0$ displays the sensitivity of the derived $q_0$ to errors in the mean absolute magnitude. Residuals for the case (3C 295 in, no evolution), which are typical, are histogramed in

TABLE 6

FINAL RESULTS

| Evolution | 3C 295 | $q_0$ | $\sigma_{q_0}$ | $\sigma_{q_0}$ ($\mu_0$ fixed) | $\sigma_\mu$ | $\mu_0$ | $dq_0/d\mu_0$ |
|---|---|---|---|---|---|---|---|
| None..... | in | 0.31 | 0.68 | 0.49 | 0.410 | 21.19 | 6.3 |
| None..... | out | −0.15 | 0.57 | 0.42 | 0.396 | 21.15 | 5.5 |
| $x = 2$ ..... | in | −0.43 | 0.54 | 0.40 | 0.412 | 21.20 | 5.0 |
| $x = 2$ ..... | out | −1.27 | 0.56 | 0.46 | 0.380 | 21.20 | 3.8 |

figure 5. It is instructive that the mean absolute magnitude in each case for the low-redshift sample agrees with the fitted mean to 0.01 mag, and the residuals seen accurately normal; the third moment, in particular, is quite small.

It is difficult to draw any firm conclusions from this body of data; the uncertainties are still too large. The classical steady state ($q_0 = -1$, no evolution in the mean) still seems very unlikely, though it is less than 2 $\sigma$ away from the fit for the sample with 3C 295 excluded. The large negative values of $q_0$ demanded by Lemaître models also stretch the statistics unless the evolutionary corrections are very large. Dense universes are also excluded: $q_0 = 2$ is more than 2 $\sigma$ away from any fit, with or without evolution; $q_0 = 1$ is at least 2 $\sigma$ away from the fit for all cases except 3C 295 in, no evolution.

It is interesting that half of the error in $q_0$ for the present sample is contributed by the inexactness of our knowledge of $\mu_0$ (the formal variance for $q_0$ with fixed $\mu_0$ is approximately half the formal variance for determination of both; cf. eq. [30] and table 6). Thus one need is more photometry of nearby clusters; it would be most satisfactory to have measurements for all of the Abell (1958) statistical sample clusters of distance class 4 or nearer, some 100 objects. Quantitative studies of these clusters can also contribute to one usable ploy to reduce the dispersion in absolute magnitude, namely, the correlation found by Bautz and Morgan (1970) and also studied by Bautz and Abell (1972) and by Sandage and Hardy (1973) between the brightness of the brightest member and the contrast between the brightest member and the rest of the cluster population. This discriminant can be applied without bias to clusters at all distances, so long as some members besides the brightest member can be seen—without which, of course, the cluster would not have been found in a purely optical survey. It is our opinion also that, despite many investigations, the Scott (1957) effect has not been properly laid to rest, and a larger body of data is needed to assess its significance. The conclusion of Sandage (1972*a*, 1973) and Sandage and Hardy (1973) that if it exists it is smaller than the intrinsic dispersion in brightness in any one richness class, is important, but not sufficient when differences in mean absolute magnitude smaller than this same dispersion can introduce large errors in the determination of $q_0$.

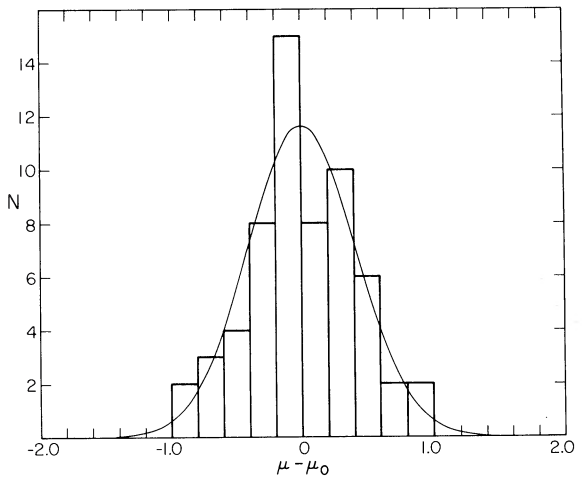


FIG. 5.—Histogram of the residuals for the fit of fig. 3. The solid curve is a Gaussian of mean 0 and the same variance as the data.

To do the job right, of course, requires data on fainter objects. The mean redshift at $S = 22.0$ for $q = \frac{1}{2}$ is about 0.60, and the separation between $q = 0$ and $q = 1$ there is 0.35 mag. Thus, 10 clusters at this brightness would separate $q = 0$ from $q = 1$ by about 3 $\sigma$. A survey aimed at this brightness level has been initiated with a 90-mm magnetic image tube at the 200-inch telescope; several clusters have been found, but too few redshift measurements have as yet been made to do meaningful statistics.

When it is all done, the results will still be meaningless without good evolutionary corrections, of course; it is hoped that work on galaxy synthesis and evolution will progress to oblige in the next few years.

The authors would like to express thanks to Drs. Maarten Schmidt (who has invented a cleverer and probably less cumbersome technique than ours for the analysis of the Hubble diagram) and Allan Sandage for enormously helpful discussions, Dr. Beatrice Tinsley for enthusiastically pursuing the evolution problem, and Gary Tuton, Dennis Palm, Juan Carrasco, and Ranney Adams, for skillful assistance at the telescopes.

This research was supported in part by National Science Foundation grants GP-31413 and GP-27304. The multichannel spectrometer was built partly and is maintained by funds provided by the National Aeronautics and Space Administration through grant NGL 05-002-134.

## REFERENCES


Abell, G. O. 1958, *Ap. J. Suppl.*, **3**, 211.
Baldwin, I. R., Danziger, I. J., Frogel, J. A., and Persson, S. E. 1973, *Ap. Letters*, **14**, 1.
Bautz, L. P., and Abell, G. O. 1972, *Bull. AAS*, **4**, 239.
Bautz, L. P., and Morgan, W. W. 1970, *Ap. J.* (*Letters*), **162**, L149.
Cramér, Harald. 1958, *Mathematical Methods of Statistics* (Princeton: Princeton University Press).
Humason, M. L., Mayall, N. U., and Sandage, A. R. 1956, *A.J.*, **61**, 97.
Humason, M. L., and Sandage, A. R. 1957, in *Carnegie Yrb., 1956* (Washington: Carnegie Institute of Washington), p. 61.
Malmquist, K. G. 1924, *Medd. Lunds Astr. Obs.*, Ser. 2, **32**, 64.
Minkowski, R. 1960, *Ap. J.*, **132**, 908.
Morgan, W. W., and Lesh, J. R. 1965, *Ap. J.*, **142**, 1364.
Oke, J. B. 1969, *Pub. A.S.P.*, **81**, 11.
———. 1971, *Ap. J.*, **170**, 193.
Oke, J. B., and Schild, R. E. 1970, *Ap. J.*, **161**, 1015.
Peterson, B. A. 1970, *A.J.*, **75**, 695.
Sandage, A. R. 1961*a*, *Ap. J.*, **133**, 355.
Sandage, A. R. 1961*b*, *Ap. J.*, **134**, 916.
———. 1972*a*, *ibid.*, **178**, 1.
———. 1972*b*, *ibid.*, p. 25.
———. 1973, *ibid.*, **183**, 731.
Sandage, A. R., and Hardy, E. 1973, *Ap. J.*, **183**, 743.
Schild, R. E., and Oke, J. B. 1971, *Ap. J.*, **169**, 209.
Scott, E. L. 1957, *A.J.*, **62**, 248.
Spinrad, H. 1972, *Ap. J.*, **171**, 463.
Tinsley, B. M. 1972*a*, *Ap. J.* (*Letters*), **178**, L39.
———. 1972*b*, *Ap. J.*, **178**, 319.
———. 1973, *Ap. J.* (*Letters*), **184**, L41.
Weinberg, S. 1972, *Gravitation and Cosmology* (New York: Wiley).
Whitford, A. E. 1958, *A.J.*, **63**, 201.
———. 1972, *Bull. AAS*, **4**, 230.
Zwicky, F. 1959, in *Handbuch der Physik*, Vol. **53**, ed. S. Flügge (Berlin: Springer-Verlag), p. 390.
Zwicky, F., Karpowicz, M., and Kowal, C. T. 1965, *Catalogue of Galaxies and of Clusters of Galaxies*, Vol. **5** (Pasadena: California Institute of Technology).


J. E. GUNN and J. B. OKE: California Institute of Technology, 1201 E. California Boulevard, Pasadena, CA 91109

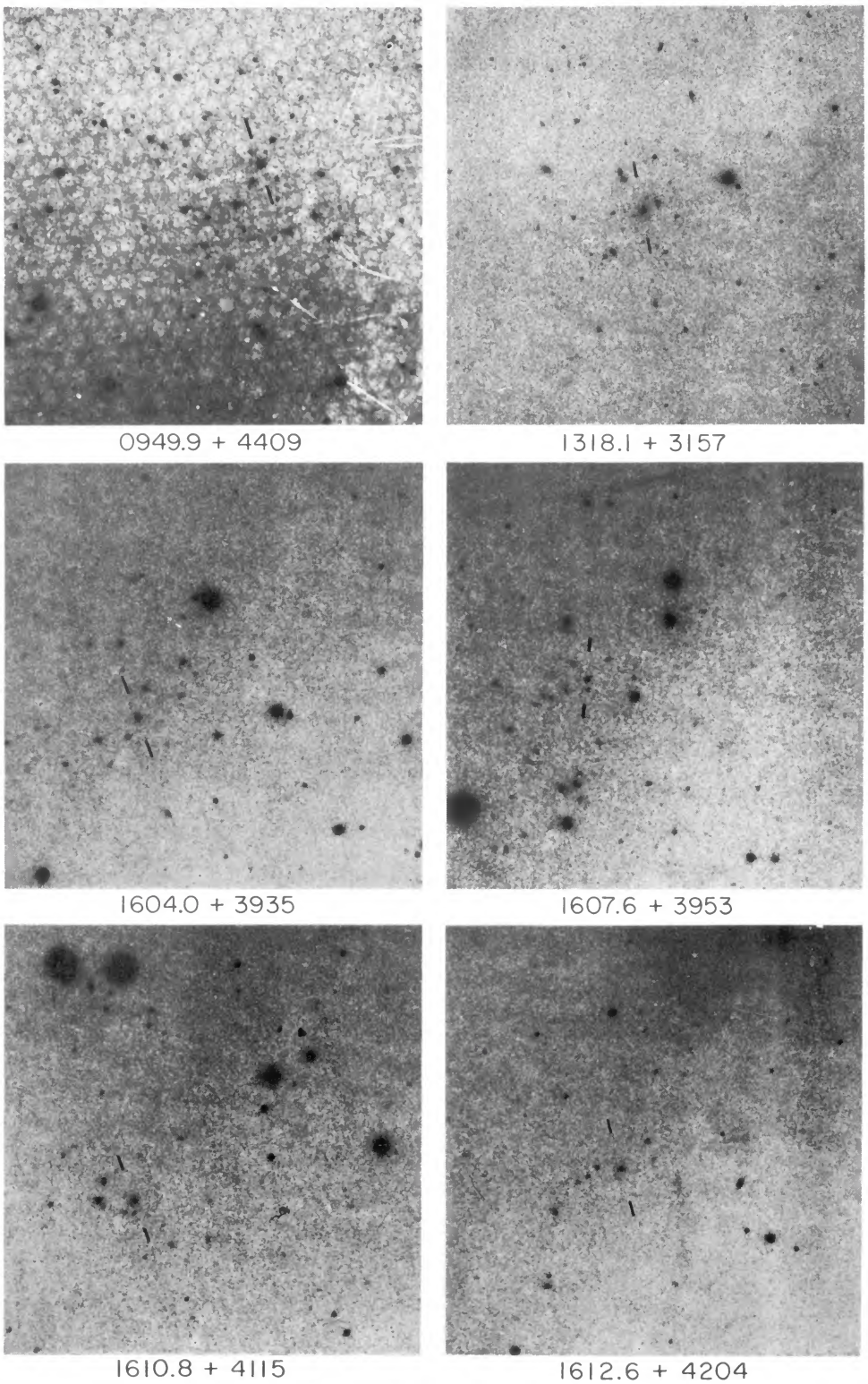


FIG. 1.—Six distant clusters. All plates were taken with a single-stage ITT 4089 or 4092 S-25 image tube with a filter which passes the region 6000–7000 Å. North is at the top, and west is at the right; each square is 4'.5 on a side.

GUNN AND OKE (*see* page 255)